SUPPORTING INFORMATION

Syngas Production from Phenolic Pollutants via A Series of Hydroxylation, Ring Cleavage, and Aqueous-Phase Reforming Catalyzed by Hydrotalcite-Supported Fe-Mn-Ni Alloy

Hanifrahmawan Sudibyo[a,b,*], Daniela V. Cabrera[c], Rodrigo Labatut[c], Calvin J. Supriyanto[a], Budhijanto Budhijanto[a], Adhika Widyaparaga[b,d]

[a]Chemical Engineering Department, Universitas Gadjah Mada, Yogyakarta 55281, Indonesia

[b]Center for Energy Studies, Universitas Gadjah Mada, Yogyakarta 55281, Indonesia

[c]Department of Hydraulic and Environmental Engineering, Pontificia Universidad Católica de Chile, Santiago 8331150, Chile

[d]Mechanical Engineering Department, Universitas Gadjah Mada, Yogyakarta 55281, Indonesia

*corresponding author: hanifrahmawan.s@ugm.ac.id

Number of figures : 21

Number of tables : 12

TABLE OF CONTENTS

Figure S1. Experimental procedures for batch experiment in the first and second stages.

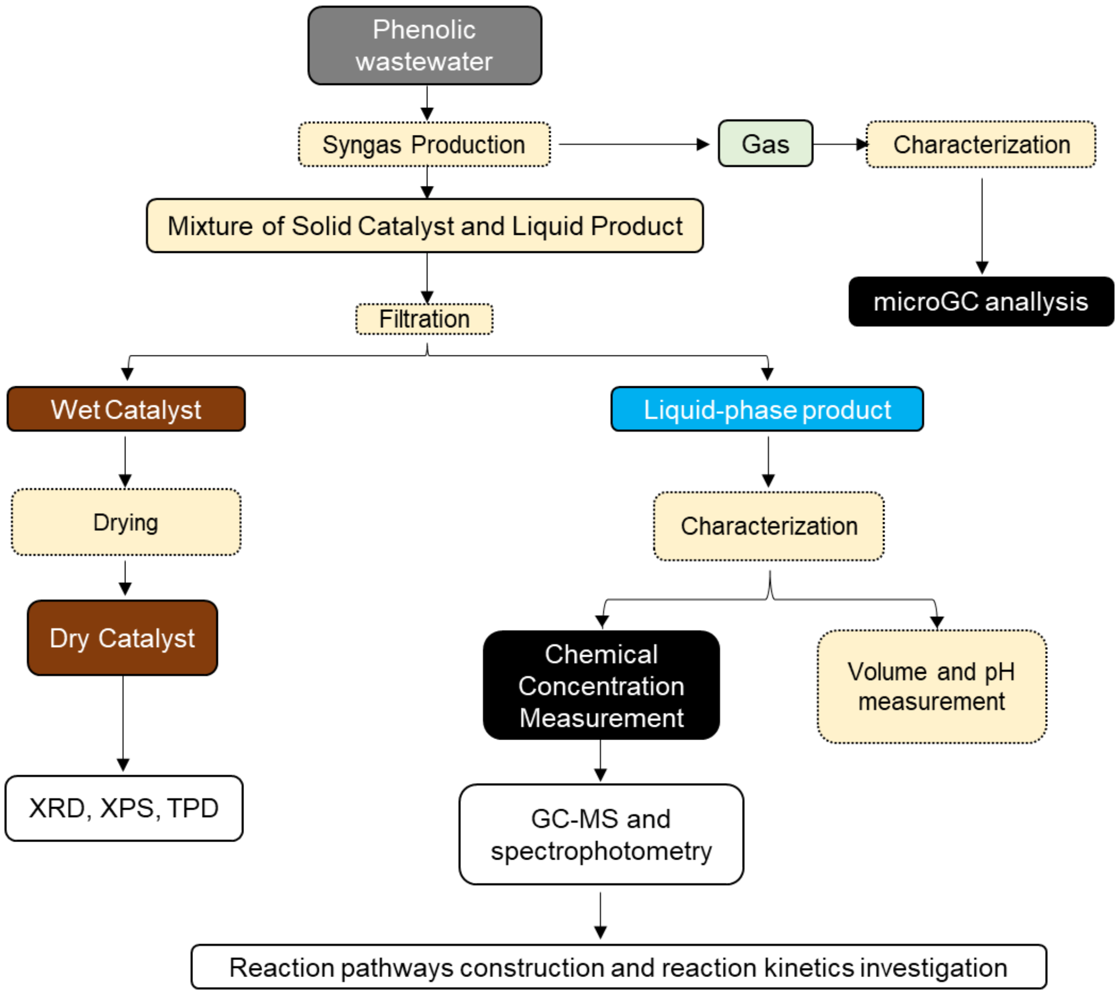

Figure S2. Experimental setup for semi-continuous experiment in the third stage.

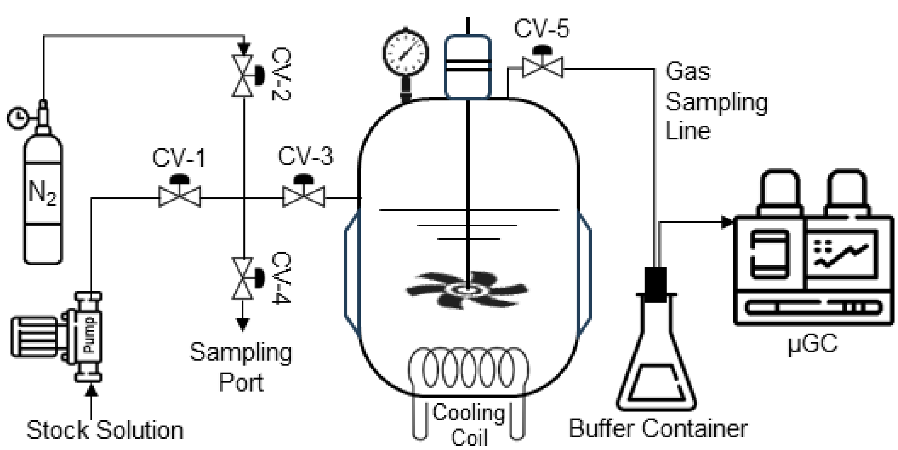

Figure S3. Pareto charts for *%TOC*$_{removal}$ from the DSD experiments. The displayed active metals are those with the highest ten counts.

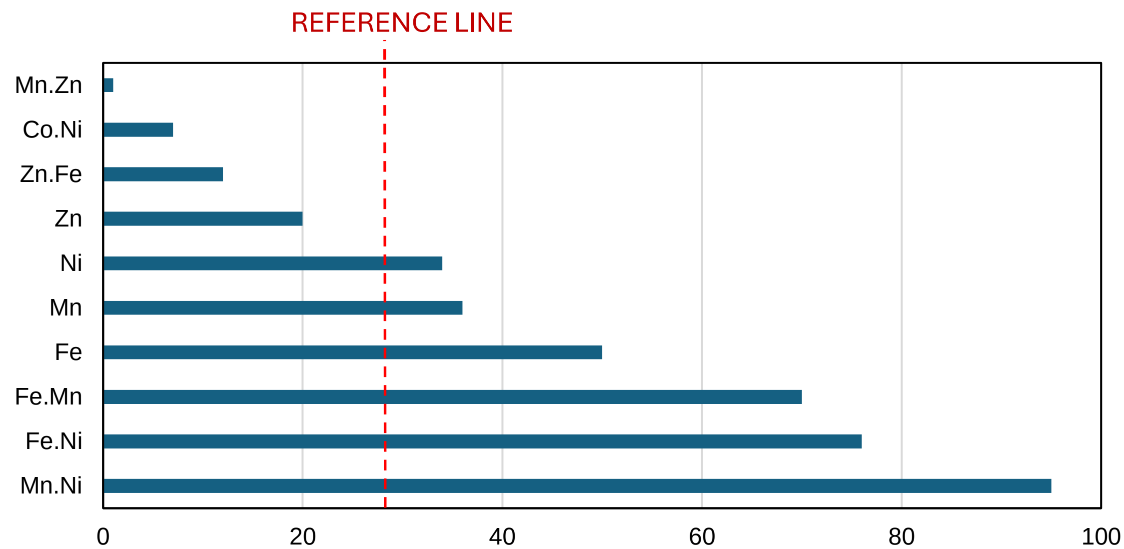

Figure S4. Pareto charts for H_2 yield from the DSD experiments. The displayed active metals are those with the highest ten counts.

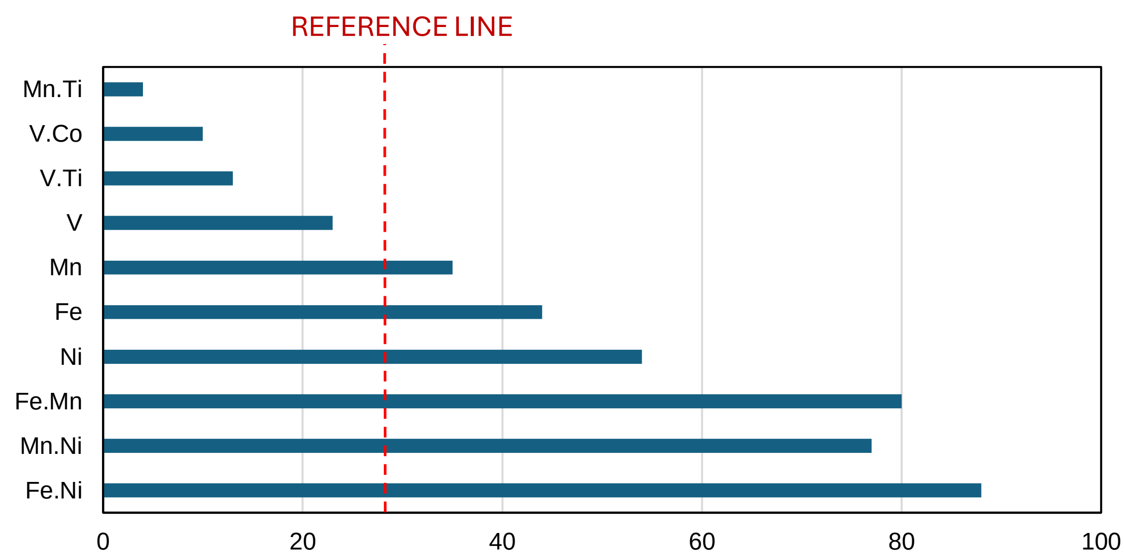

Figure S5. Pareto charts for CO:H2 molar ratio from the DSD experiments. The displayed active metals are those with the highest ten counts.

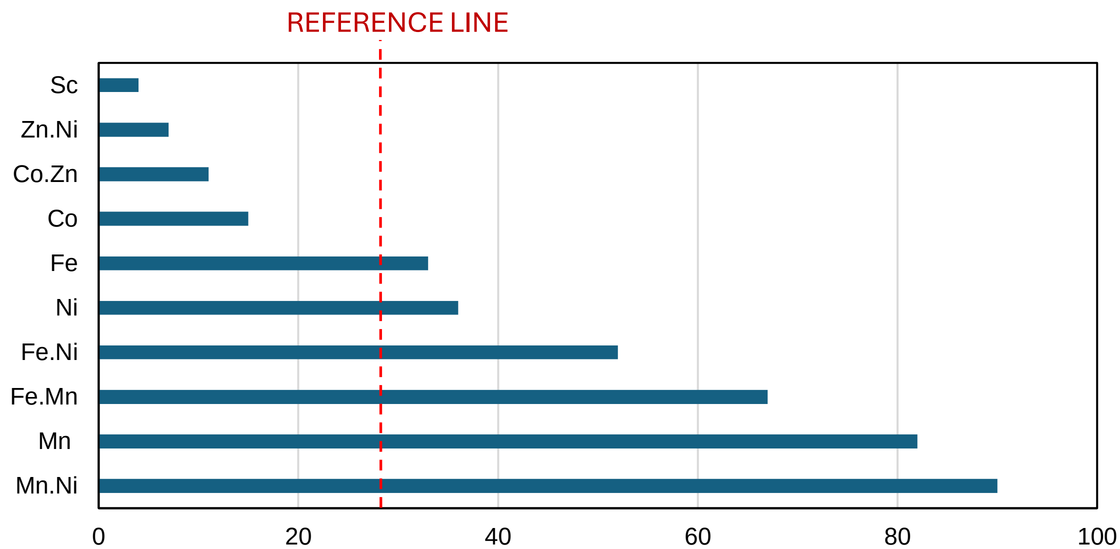

Figure S6. Pareto charts for H_2 purity in the gas product from the DSD experiments. The displayed active metals are those with the highest ten counts.

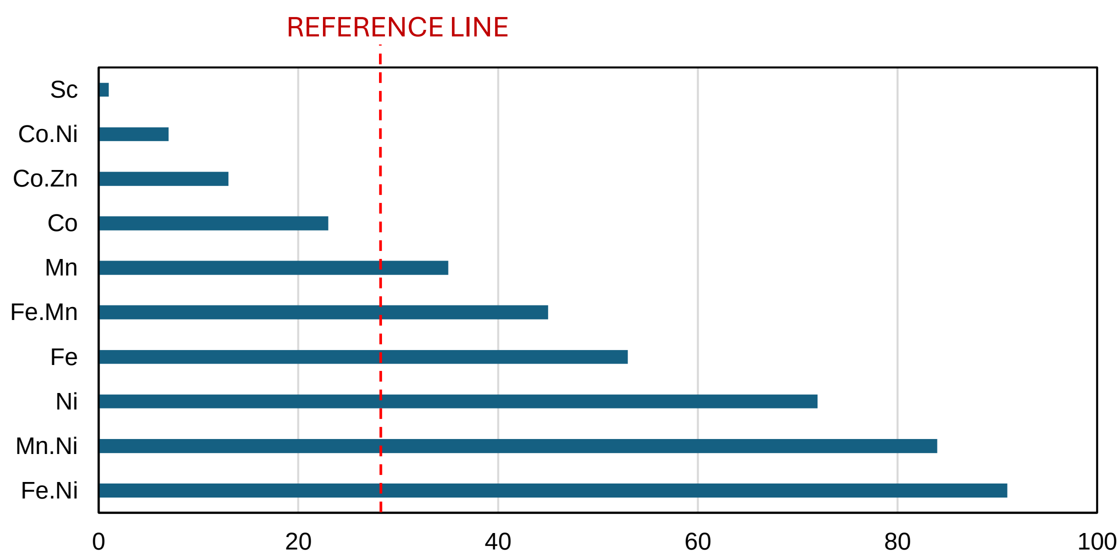

Figure S7. Pareto charts for SBrA of the catalysts whose compositions are defined in Table S2. The displayed active metals are those with the highest ten counts.

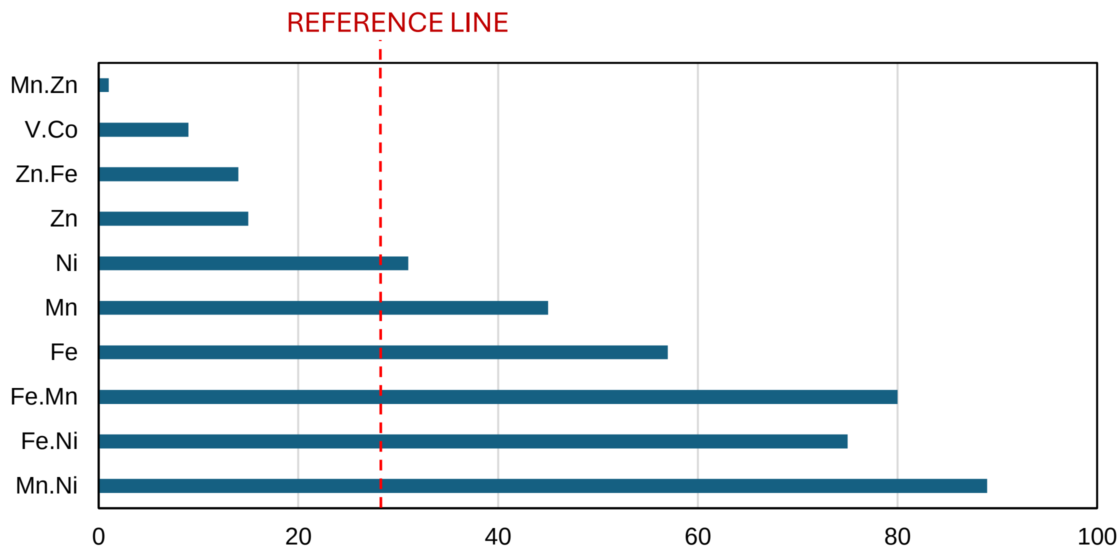

Figure S8. Pareto charts for WBrA of the catalysts whose compositions are defined in Table S2. The displayed active metals are those with the highest ten counts.

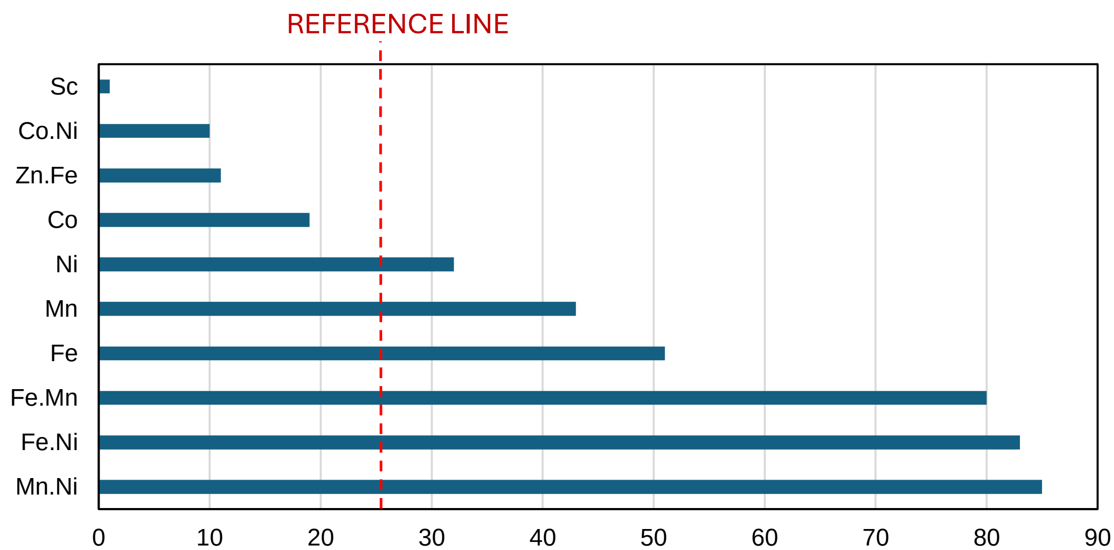

Figure S9. Pareto charts for WLA of the catalysts whose compositions are defined in Table S2. The displayed active metals are those with the highest ten counts.

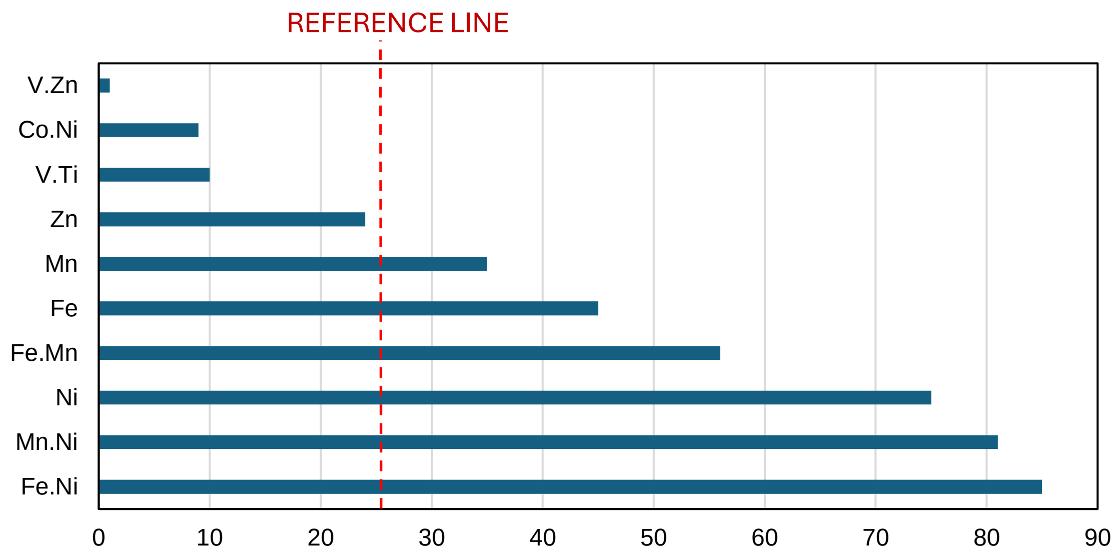

Figure S10. Pareto charts for SLA of the catalysts whose compositions are defined in Table S2. The displayed active metals are those with the highest ten counts.

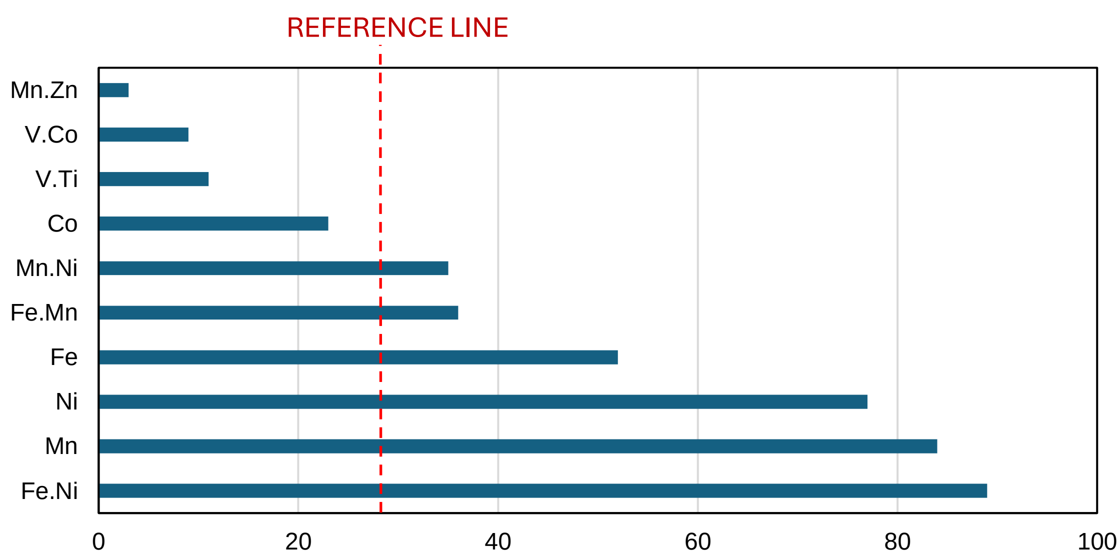

Figure S11. Pareto charts for SBS of the catalysts whose compositions are defined in Table S2. The displayed active metals are those with the highest ten counts.

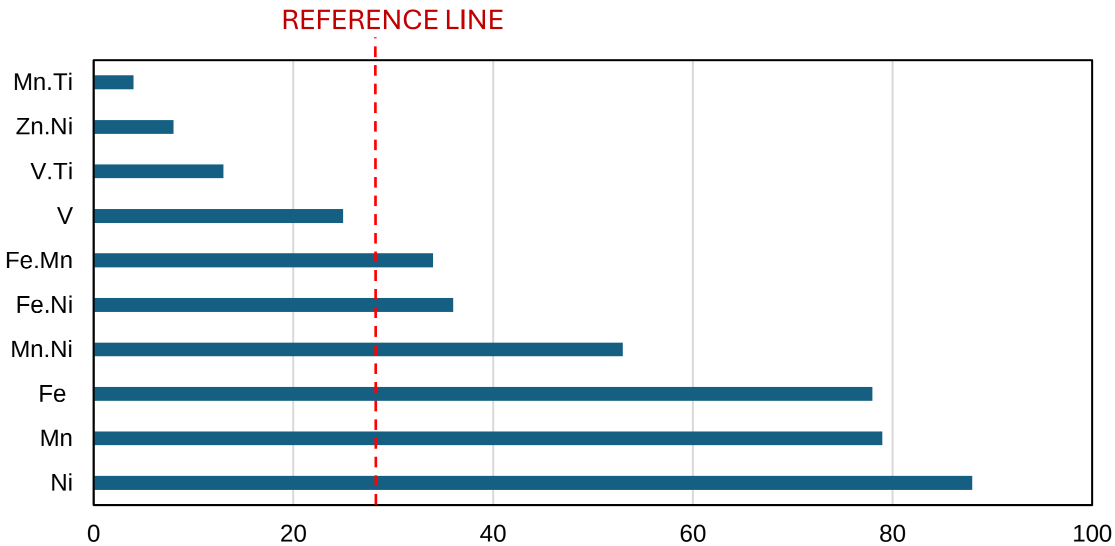

Figure S12. Pareto charts for phenols conversion. The displayed active metals are those with the highest ten counts.

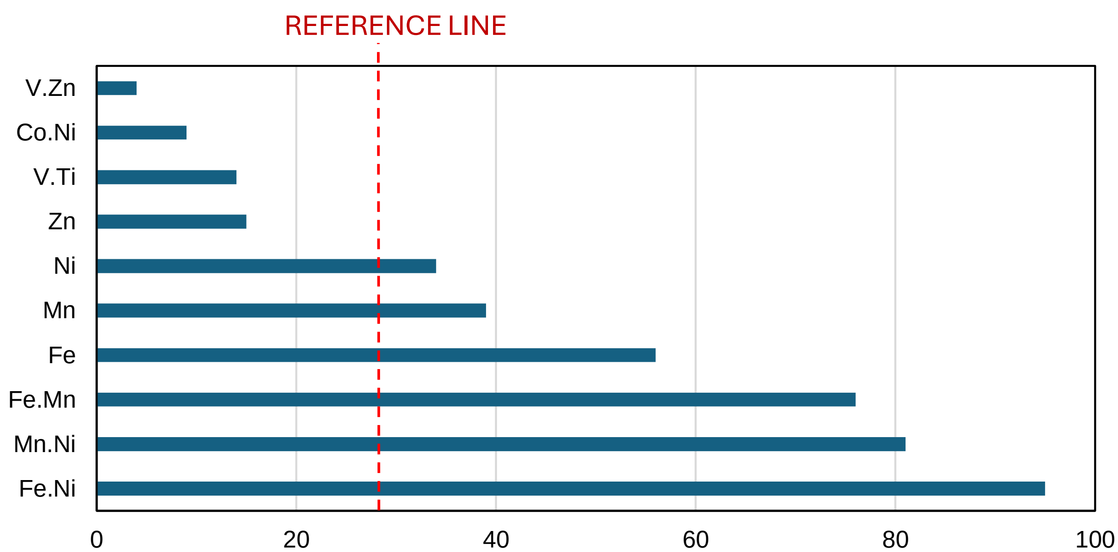

Figure S13. Pareto charts for acid content in the aqueous product. The displayed active metals are those with the highest ten counts.

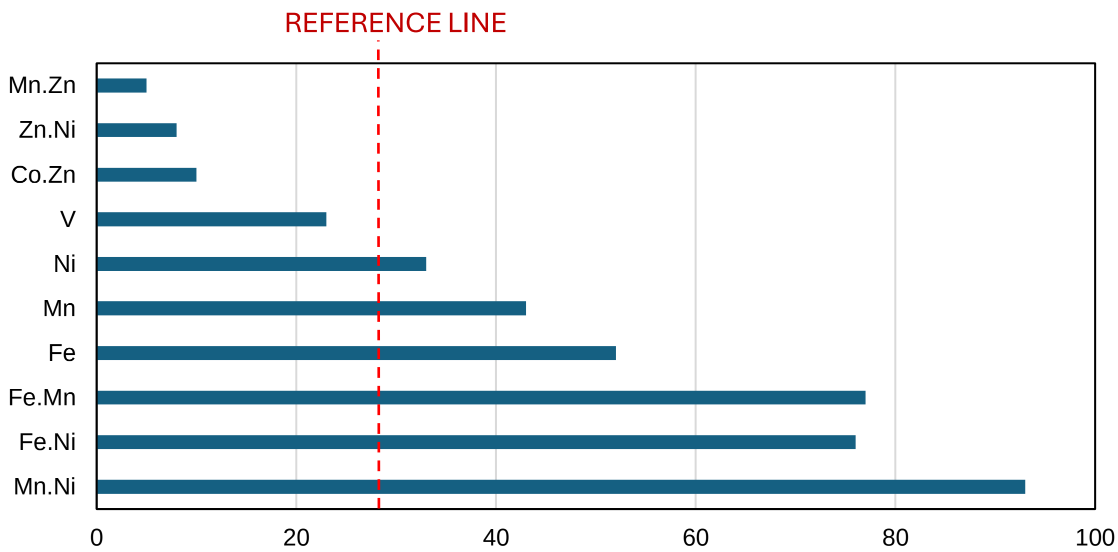

Figure S14. The TON and TOF and the *%TOC*$_{removal}$ and CO-to-H_2 ratio of the optimized Fe-Mn-Ni/HT catalysts at reaction temperature of 200 ºC.

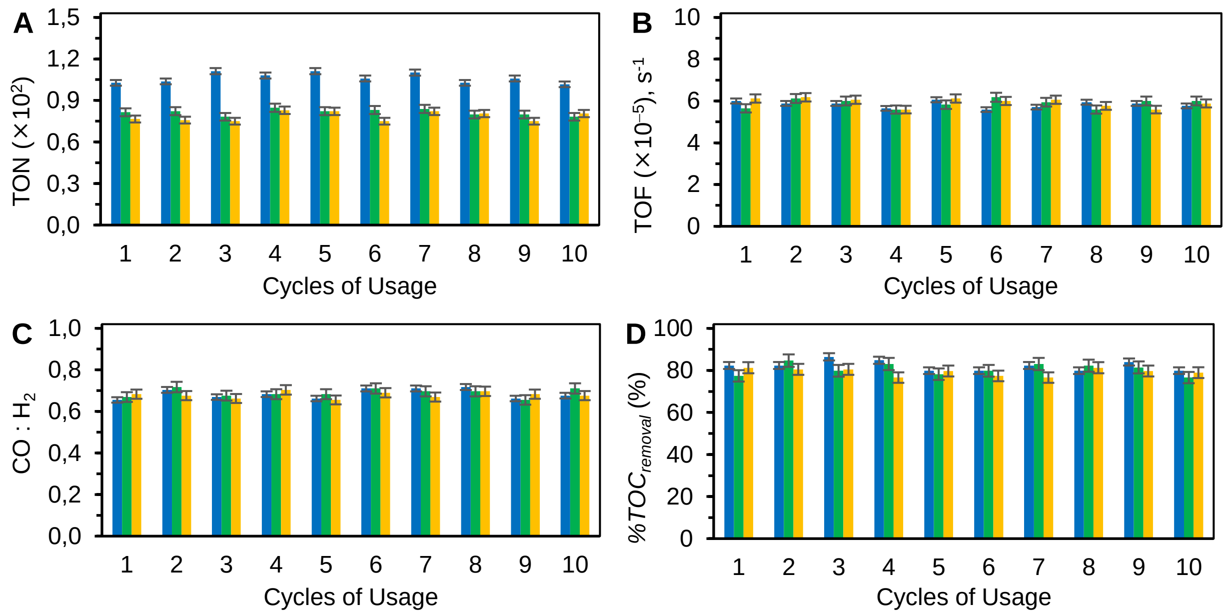

Figure S15. The TON and TOF and the *%TOC*$_{removal}$ and CO-to-H_2 ratio of the optimized Fe-Mn-Ni/HT catalysts at reaction temperature of 300 ºC.

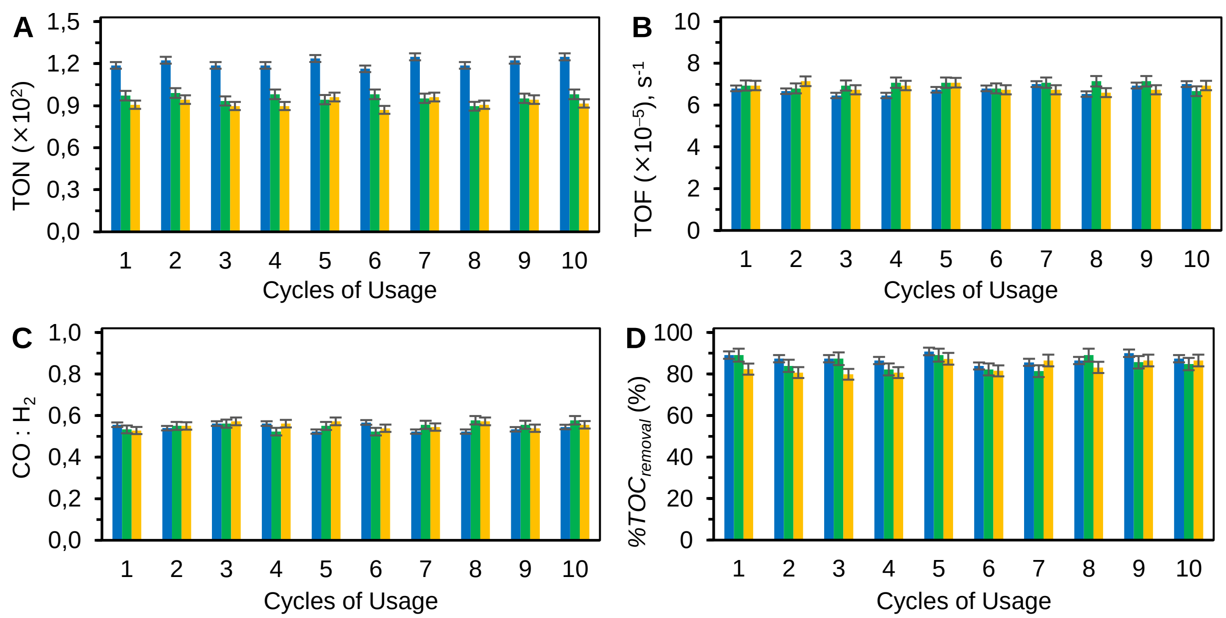

Figure S16. The XRD diffractograms for (a) hydrotalcite (HT), (b) Fe/HT, (c) Mn/HT, (d) Ni/HT, (e) Fe-Mn/HT, (f) Fe-Ni/HT, (g) Mn-Ni/HT, and (h) Fe-Mn-Ni/HT.

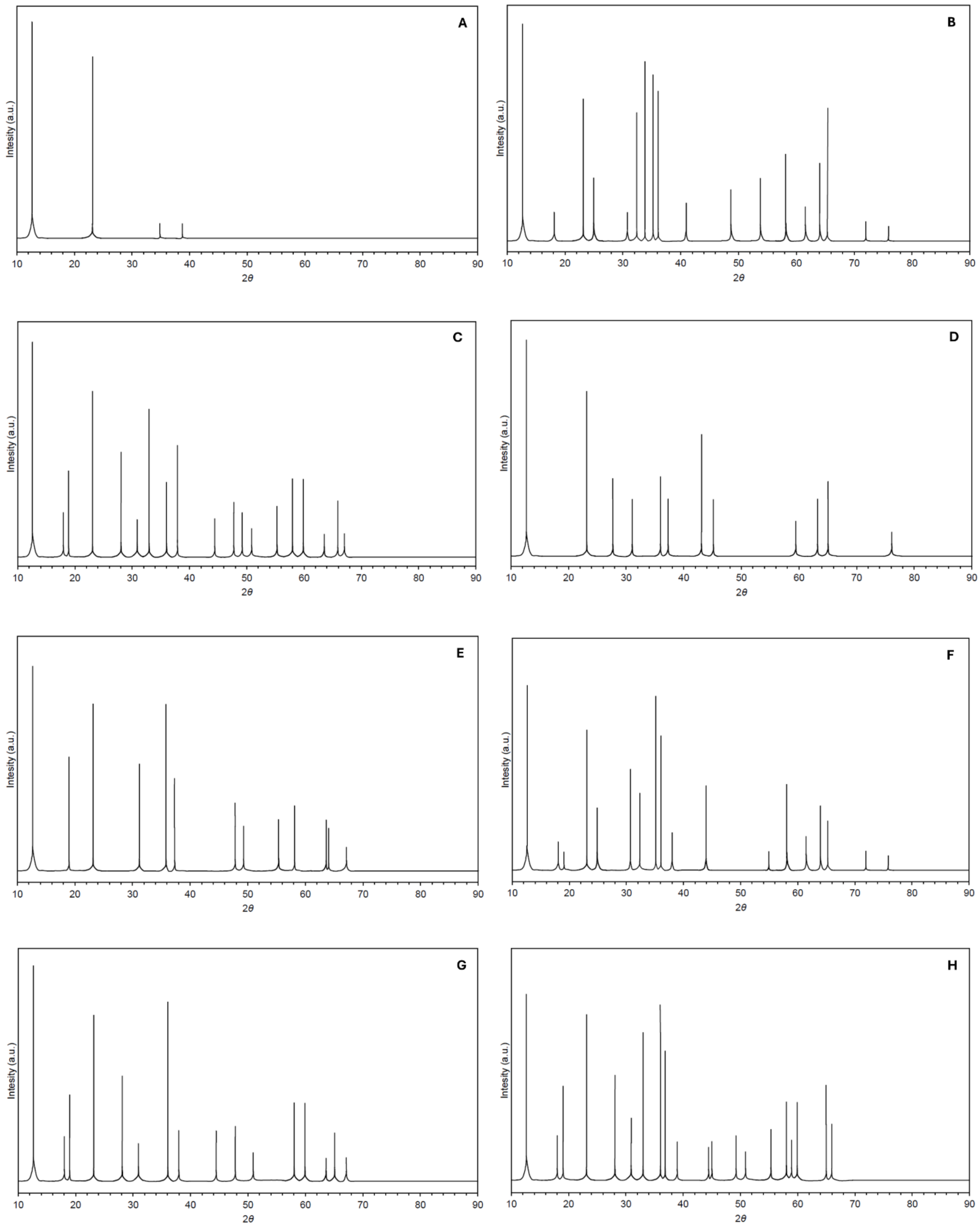

Figure S17. The XRD diffractograms for (a) Fe/HT, (b) Mn/HT, (c) Ni/HT, (d) Fe-Mn/HT, (e) Fe-Ni/HT, (f) Mn-Ni/HT, and (g) Fe-Mn-Ni/HT after being used for producing syngas.

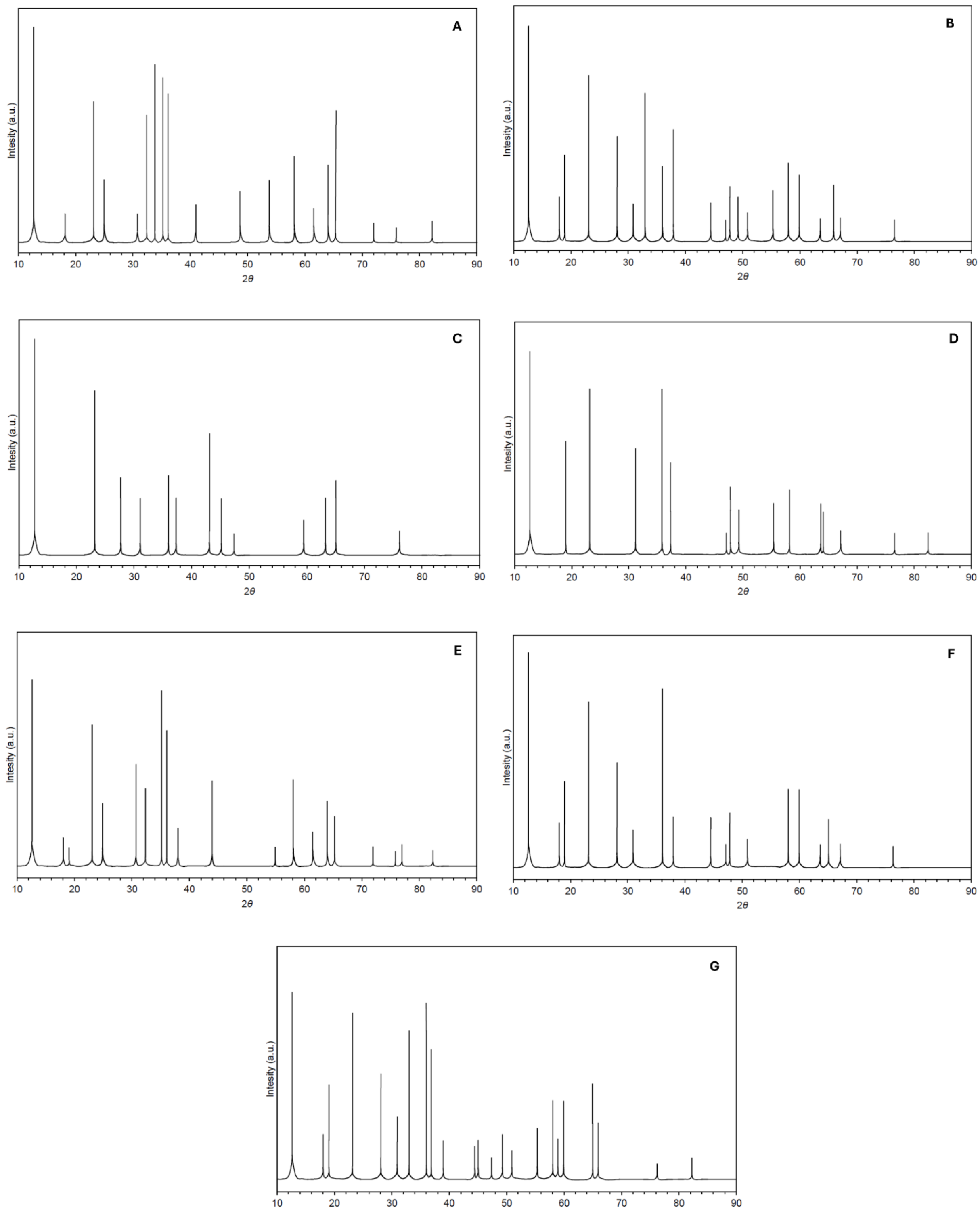

Figure S18. The N_2-BET plots for (a) hydrotalcite (HT), (b) Fe/HT, (c) Mn/HT, (d) Ni/HT, (e) Fe-Mn/HT, (f) Fe-Ni/HT, (g) Mn-Ni/HT, and (h) Fe-Mn-Ni/HT.

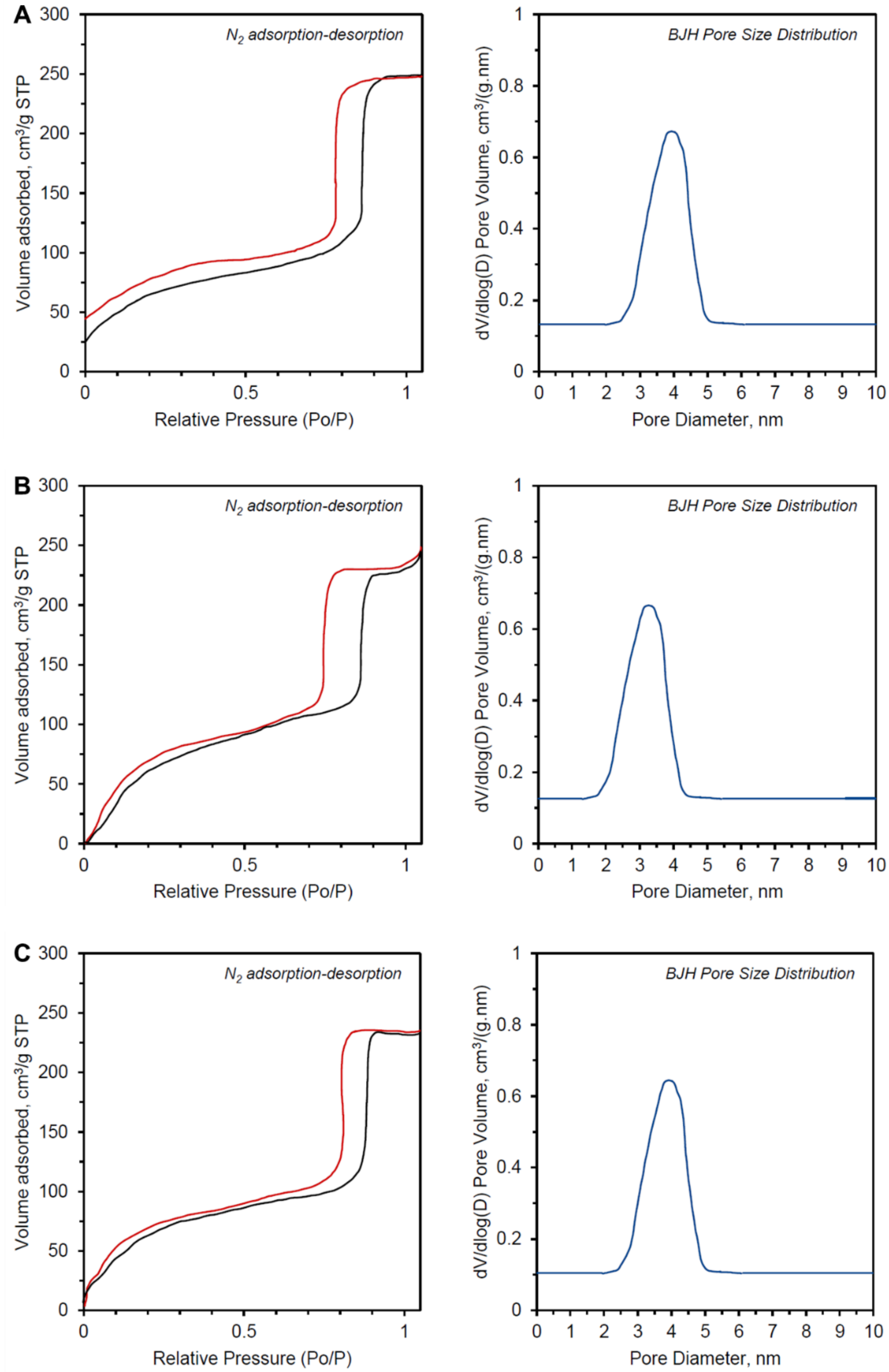

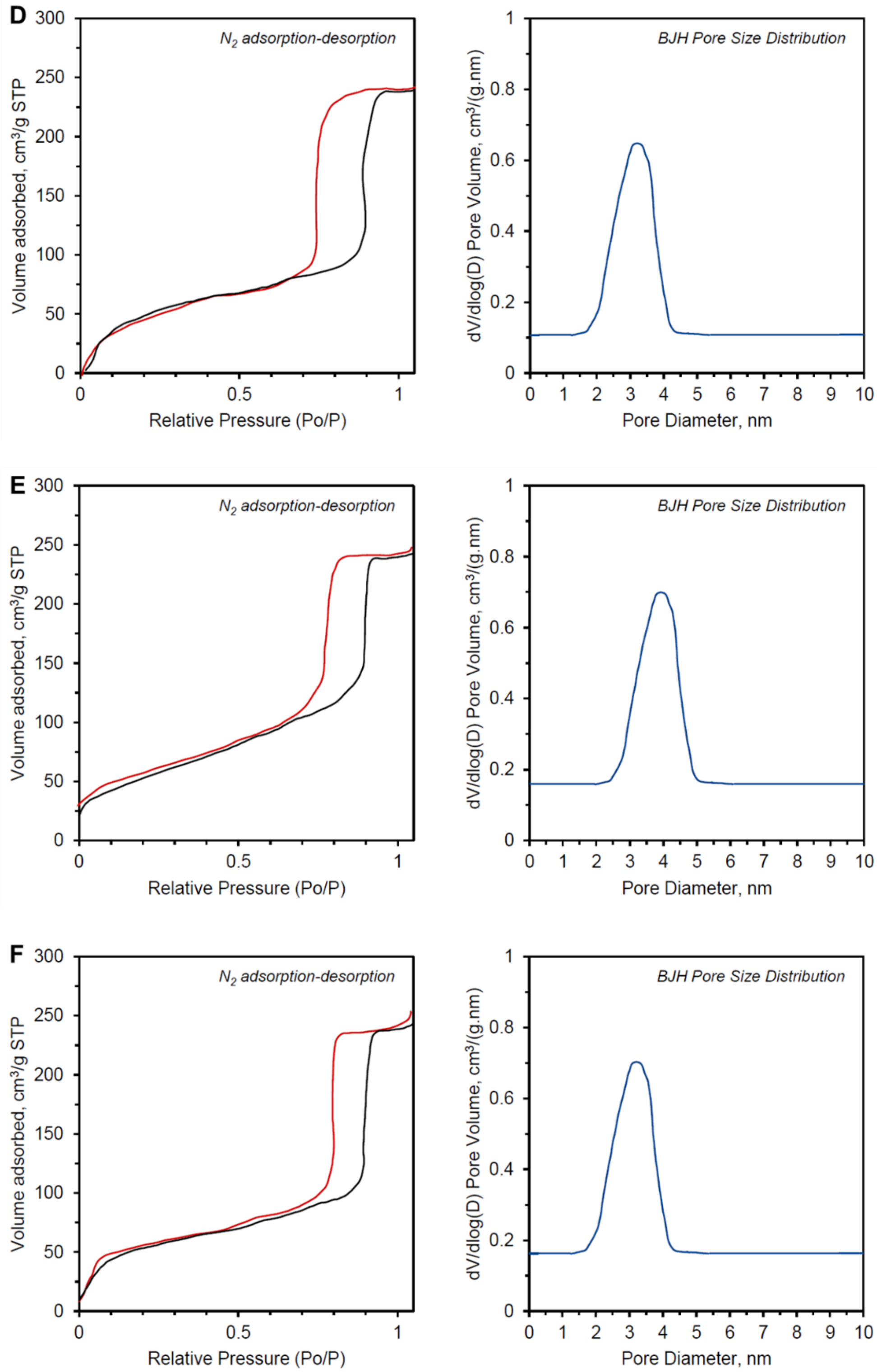
D
E
F
N2 adsorption-desorption
Volume adsorbed, cm³/g STP
Relative Pressure (Po/P)
BJH Pore Size Distribution
dV/dlog(D) Pore Volume, cm³/(g.nm)
Pore Diameter, nm
0
50
100
150
200
250
300
0.5
1
0.2
0.4
0.6
0.8
2
3
4
5
6
7
8
9
10

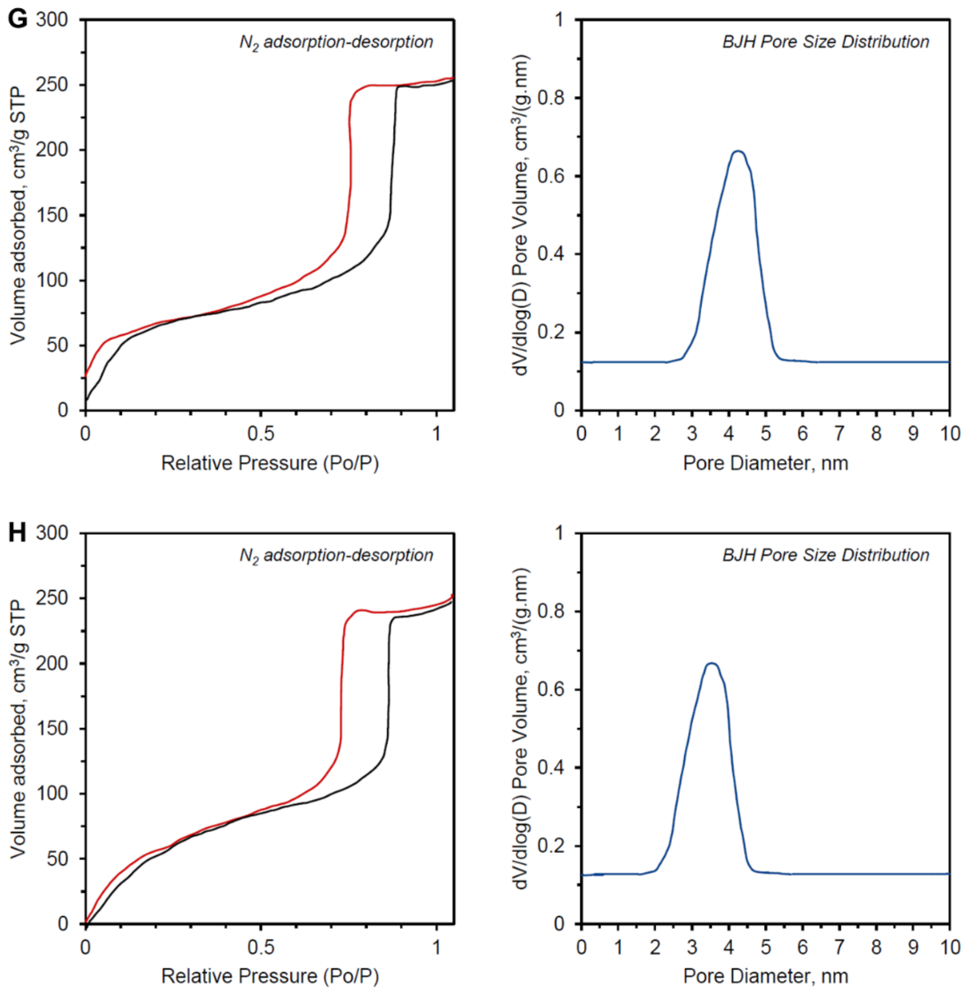

Figure S19. The N2-BET plots for (a) Fe/HT, (b) Mn/HT, (c) Ni/HT, (d) Fe-Mn/HT, (e) Fe-Ni/HT, (f) Mn-Ni/HT, and (g) Fe-Mn-Ni/HT after being used for producing syngas.

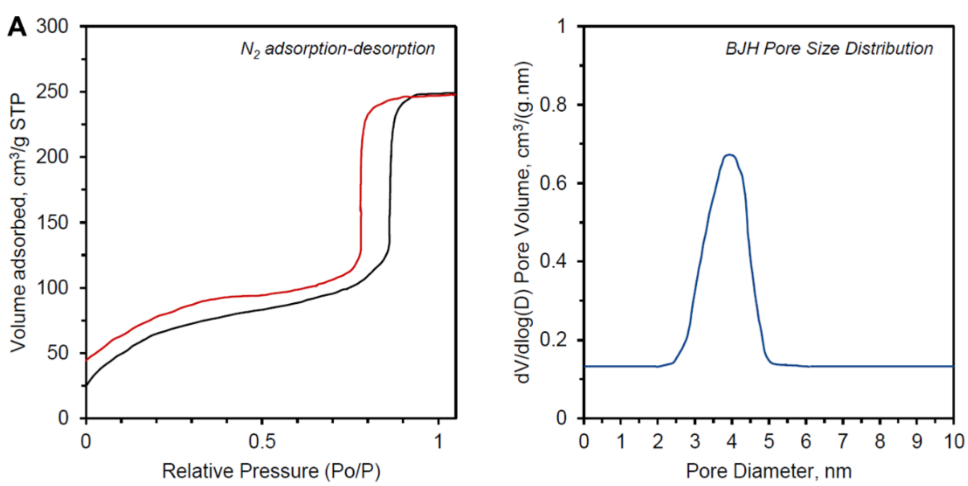

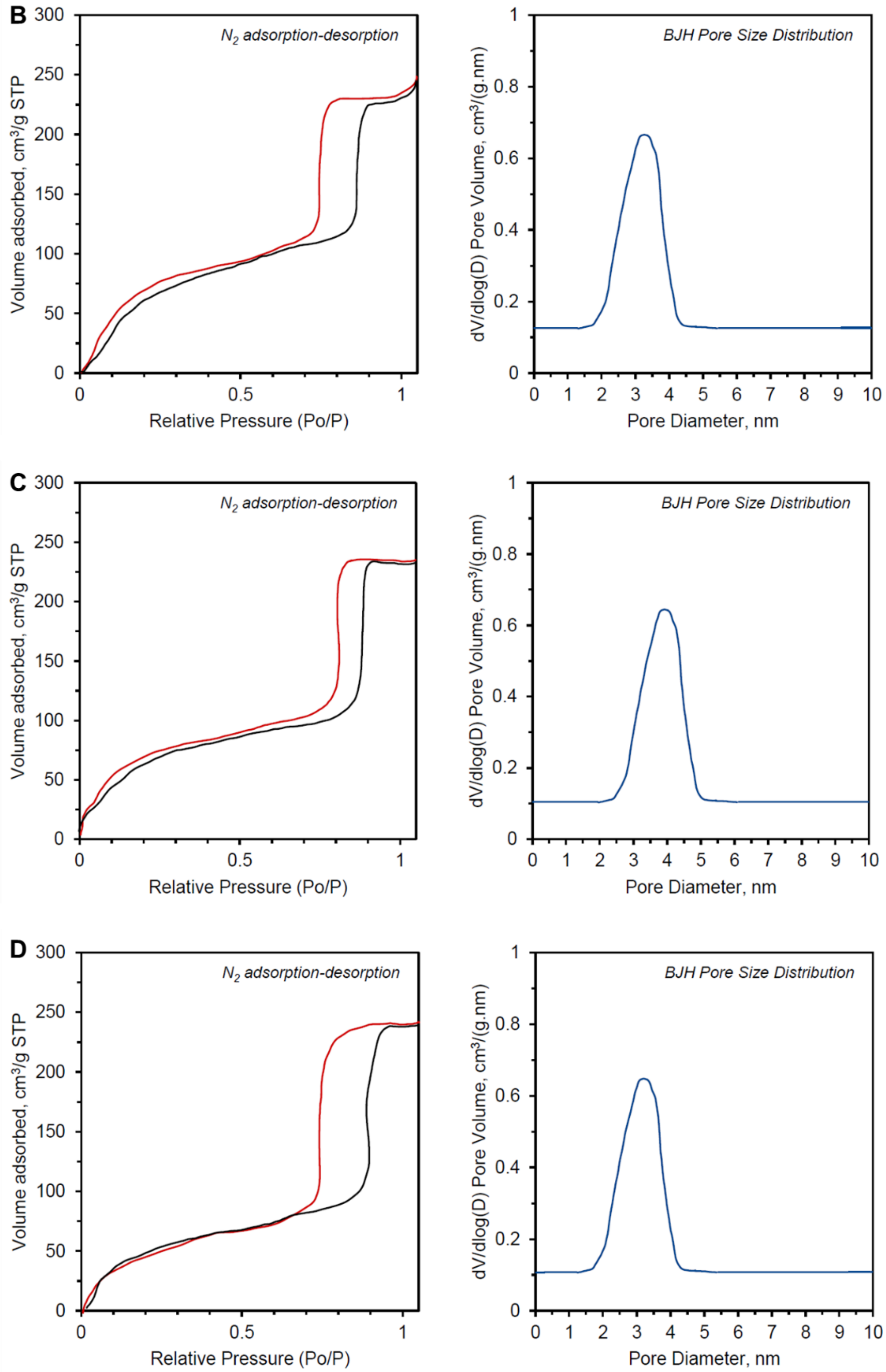
B
N2 adsorption-desorption
Volume adsorbed, cm³/g STP
Relative Pressure (Po/P)
BJH Pore Size Distribution
dV/dlog(D) Pore Volume, cm³/(g.nm)
Pore Diameter, nm
C
N2 adsorption-desorption
Volume adsorbed, cm³/g STP
Relative Pressure (Po/P)
BJH Pore Size Distribution
dV/dlog(D) Pore Volume, cm³/(g.nm)
Pore Diameter, nm
D
N2 adsorption-desorption
Volume adsorbed, cm³/g STP
Relative Pressure (Po/P)
BJH Pore Size Distribution
dV/dlog(D) Pore Volume, cm³/(g.nm)
Pore Diameter, nm

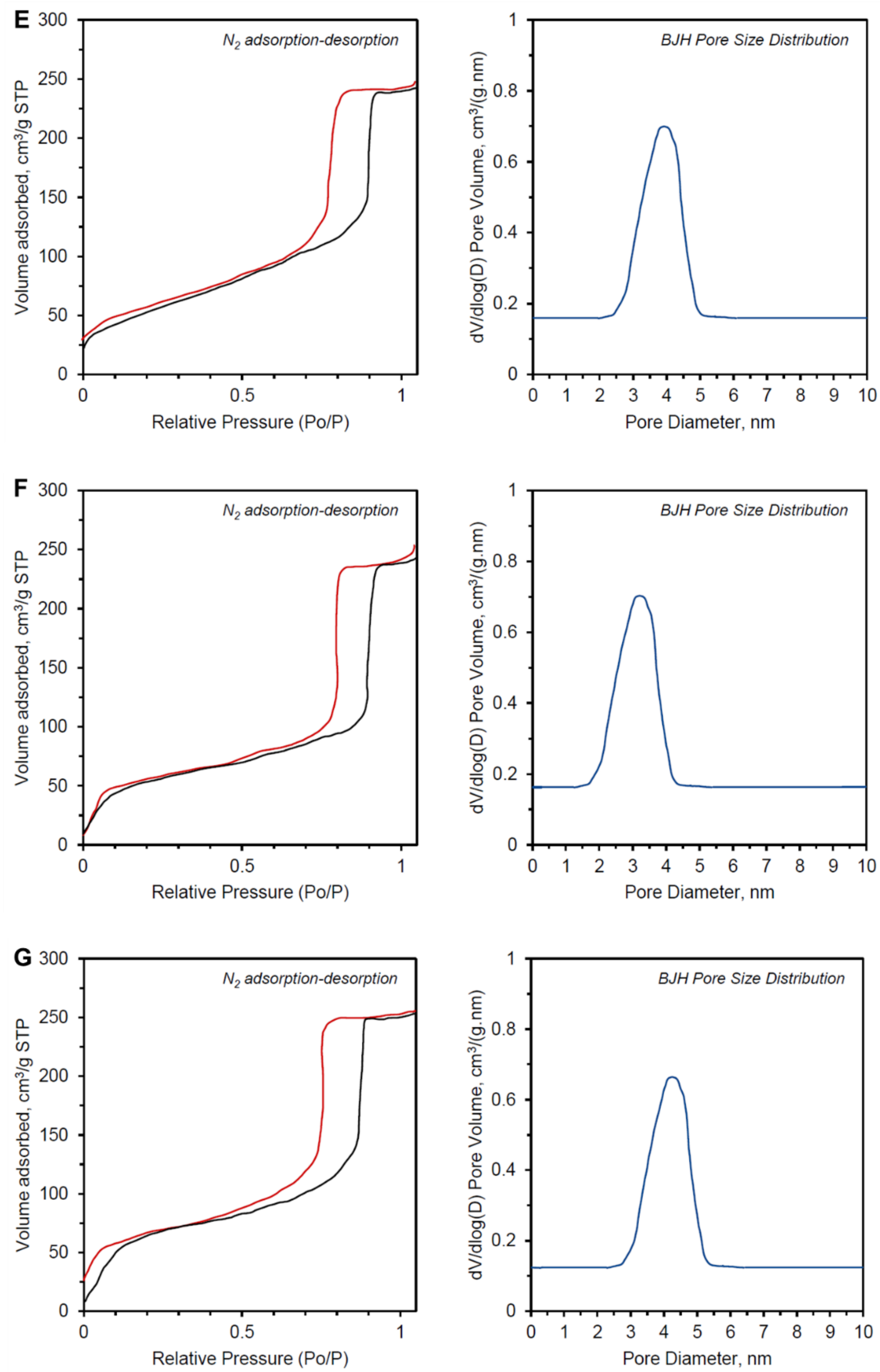
E
N2 adsorption-desorption
Volume adsorbed, cm3/g STP
Relative Pressure (Po/P)
BJH Pore Size Distribution
dV/dlog(D) Pore Volume, cm3/(g.nm)
Pore Diameter, nm
F
N2 adsorption-desorption
Volume adsorbed, cm3/g STP
Relative Pressure (Po/P)
BJH Pore Size Distribution
dV/dlog(D) Pore Volume, cm3/(g.nm)
Pore Diameter, nm
G
N2 adsorption-desorption
Volume adsorbed, cm3/g STP
Relative Pressure (Po/P)
BJH Pore Size Distribution
dV/dlog(D) Pore Volume, cm3/(g.nm)
Pore Diameter, nm

Figure S20. The NH_3-TPD and CO_2-TPD plots for (a) hydrotalcite (HT), (b) Fe/HT, (c) Mn/HT, (d) Ni/HT, (e) Fe-Mn/HT, (f) Fe-Ni/HT, (g) Mn-Ni/HT, and (h) Fe-Mn-Ni/HT.

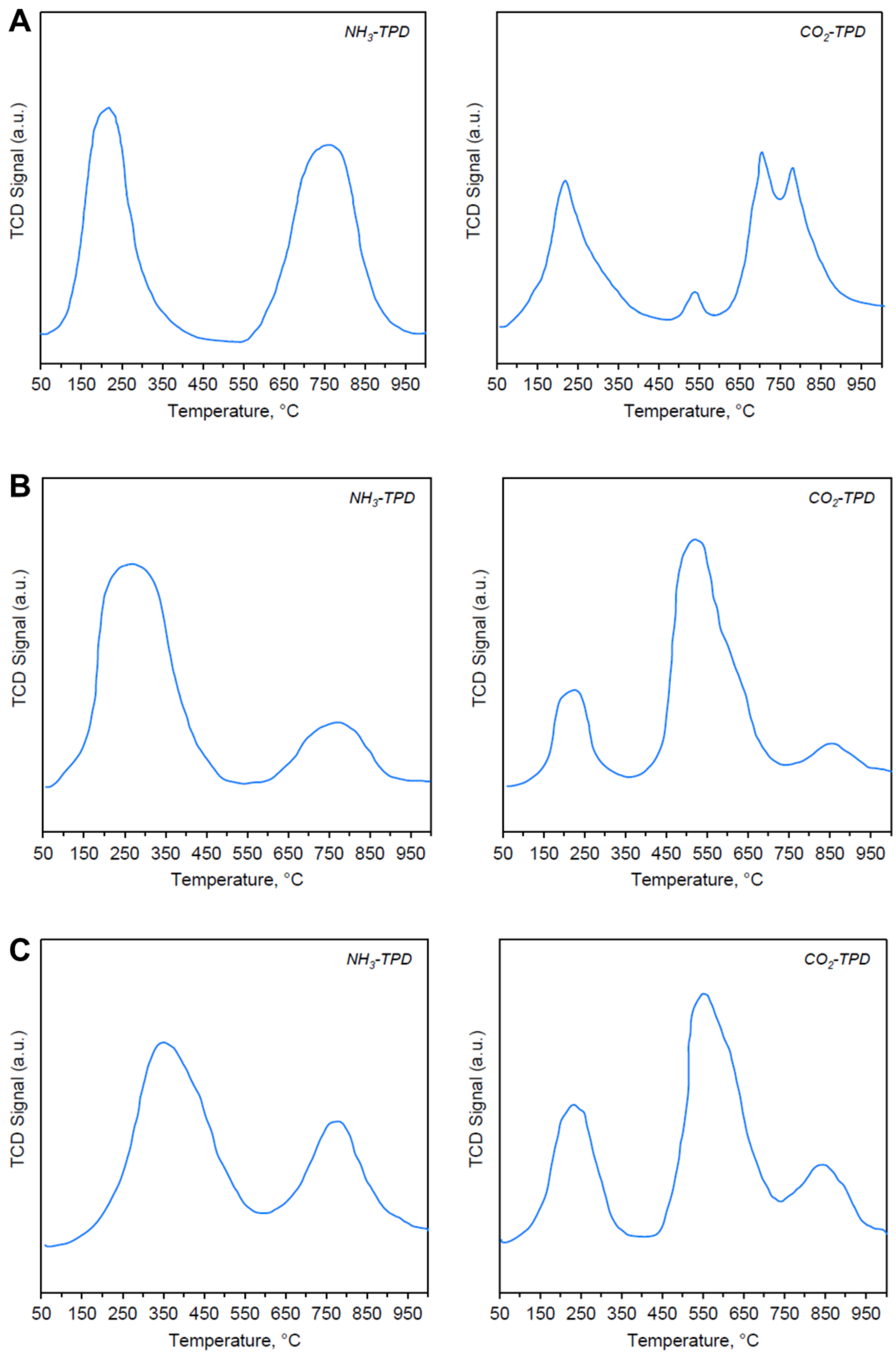

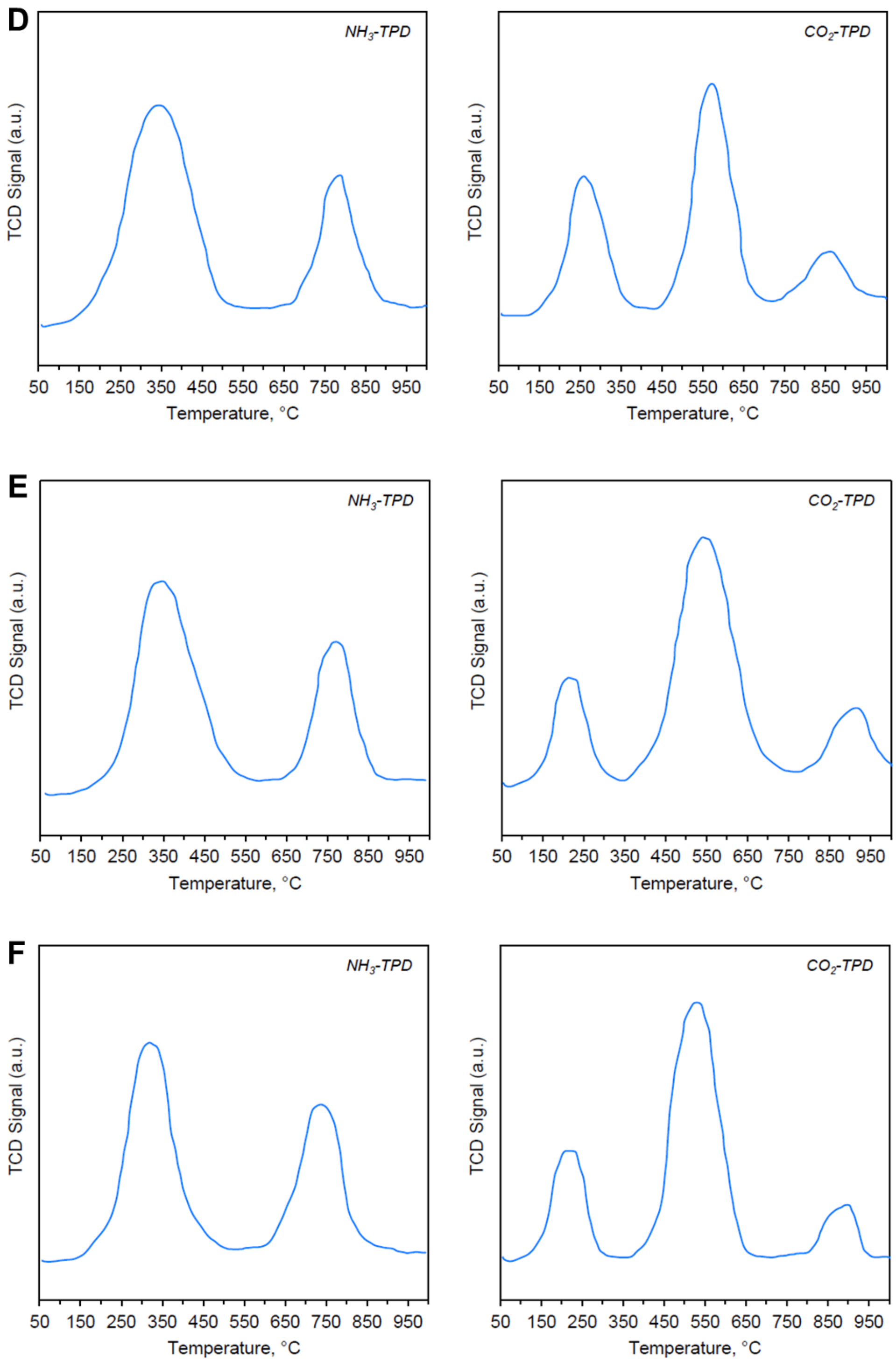
D
NH$_3$-TPD
TCD Signal (a.u.)
50 150 250 350 450 550 650 750 850 950
Temperature, °C
CO$_2$-TPD
TCD Signal (a.u.)
50 150 250 350 450 550 650 750 850 950
Temperature, °C
E
NH$_3$-TPD
TCD Signal (a.u.)
50 150 250 350 450 550 650 750 850 950
Temperature, °C
CO$_2$-TPD
TCD Signal (a.u.)
50 150 250 350 450 550 650 750 850 950
Temperature, °C
F
NH$_3$-TPD
TCD Signal (a.u.)
50 150 250 350 450 550 650 750 850 950
Temperature, °C
CO$_2$-TPD
TCD Signal (a.u.)
50 150 250 350 450 550 650 750 850 950
Temperature, °C

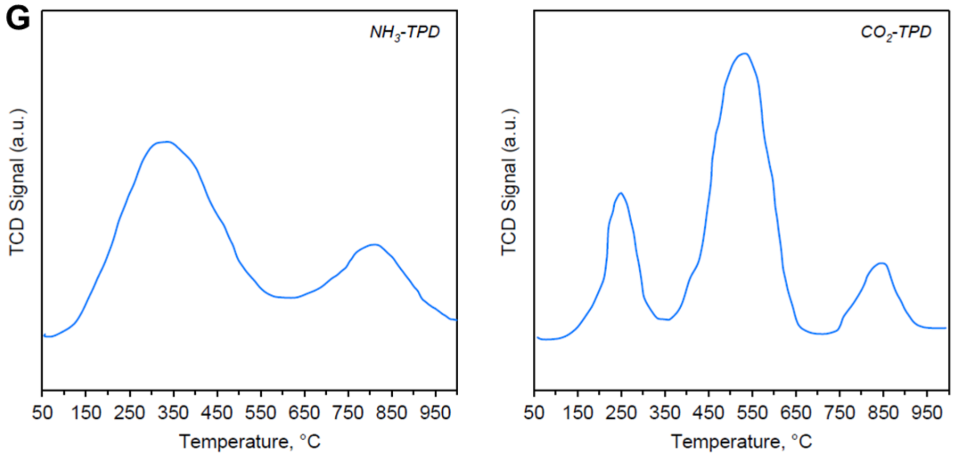

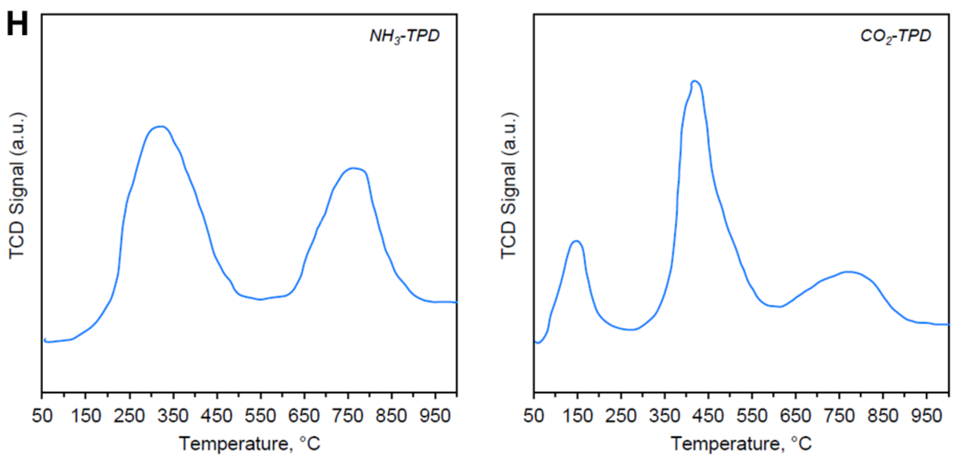

Figure S21. The NH_3-TPD and CO_2-TPD plots for (a) Fe/HT, (b) Mn/HT, (c) Ni/HT, (d) Fe-Mn/HT, (e) Fe-Ni/HT, (f) Mn-Ni/HT, and (g) Fe-Mn-Ni/HT after being used for producing syngas.

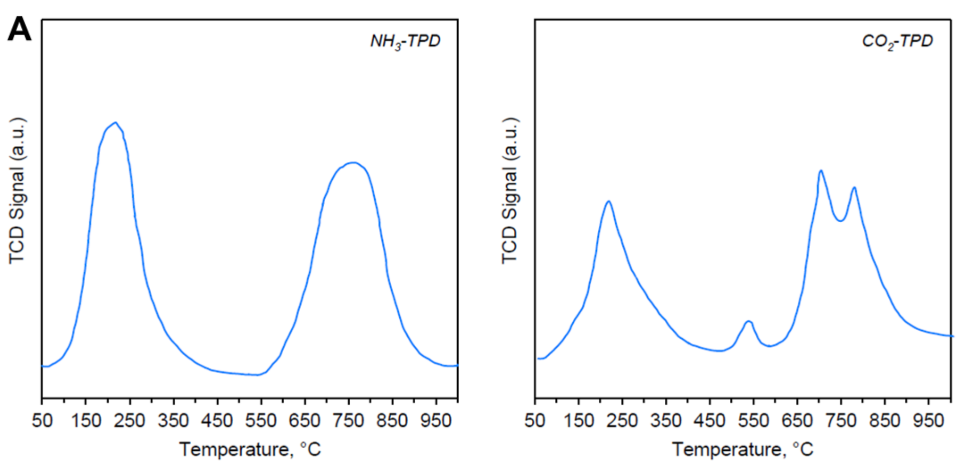

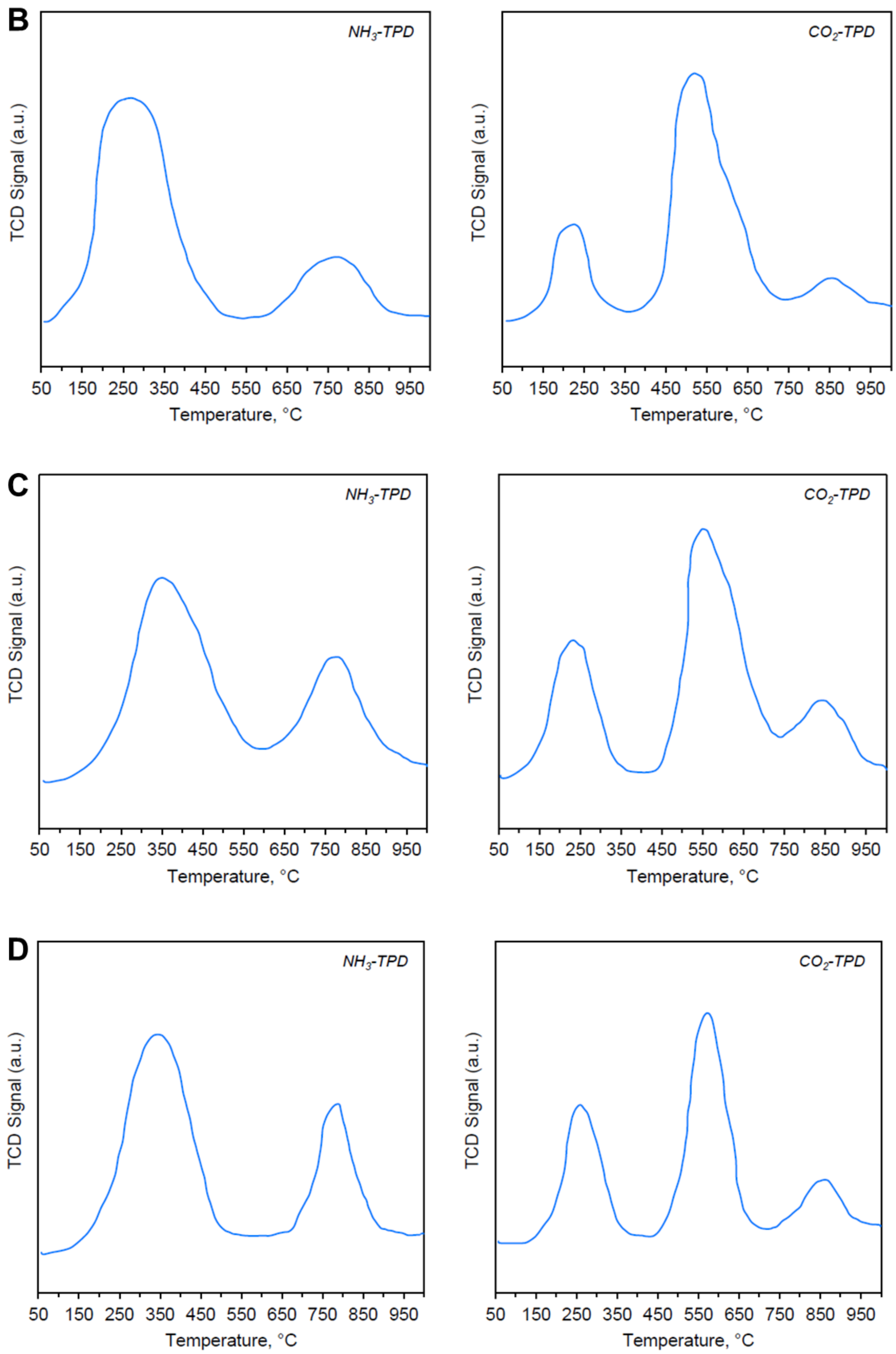
B
NH3-TPD
TCD Signal (a.u.)
50 150 250 350 450 550 650 750 850 950
Temperature, °C
CO2-TPD
TCD Signal (a.u.)
50 150 250 350 450 550 650 750 850 950
Temperature, °C
C
NH3-TPD
TCD Signal (a.u.)
50 150 250 350 450 550 650 750 850 950
Temperature, °C
CO2-TPD
TCD Signal (a.u.)
50 150 250 350 450 550 650 750 850 950
Temperature, °C
D
NH3-TPD
TCD Signal (a.u.)
50 150 250 350 450 550 650 750 850 950
Temperature, °C
CO2-TPD
TCD Signal (a.u.)
50 150 250 350 450 550 650 750 850 950
Temperature, °C

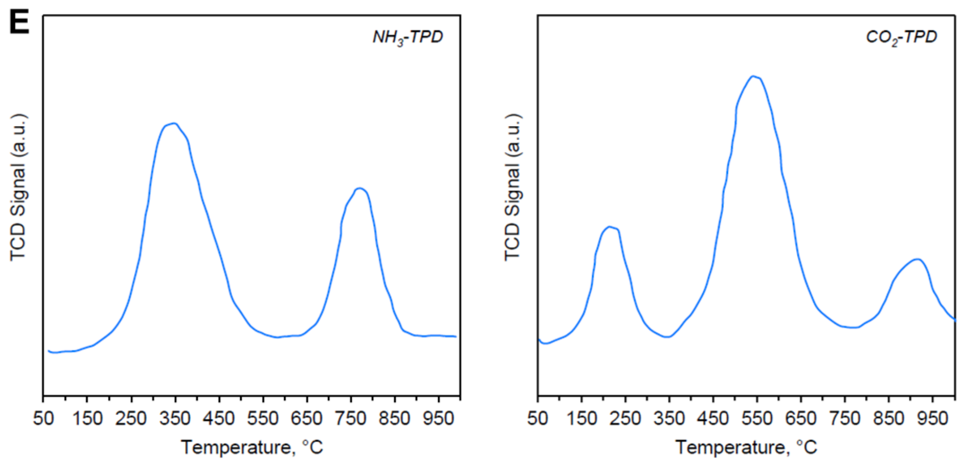
E
NH_3-TPD
TCD Signal (a.u.)
50 150 250 350 450 550 650 750 850 950
Temperature, °C
CO_2-TPD
TCD Signal (a.u.)
50 150 250 350 450 550 650 750 850 950
Temperature, °C

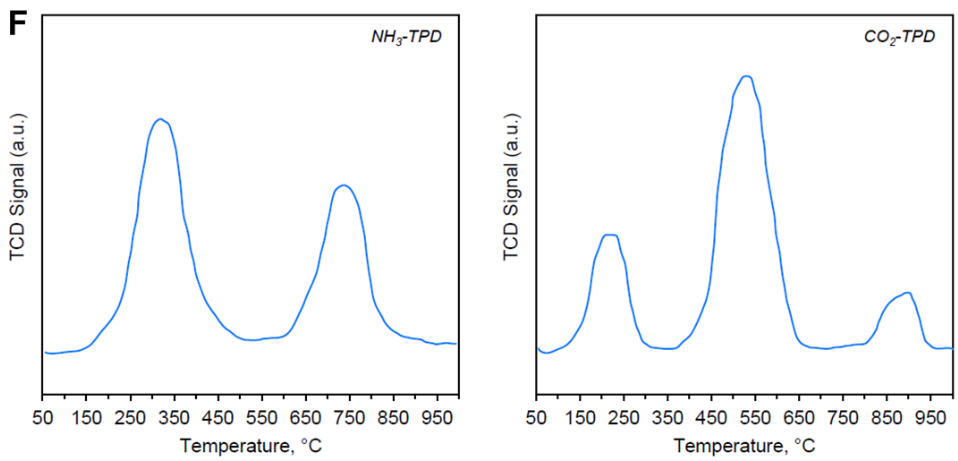
F
NH_3-TPD
TCD Signal (a.u.)
50 150 250 350 450 550 650 750 850 950
Temperature, °C
CO_2-TPD
TCD Signal (a.u.)
50 150 250 350 450 550 650 750 850 950
Temperature, °C

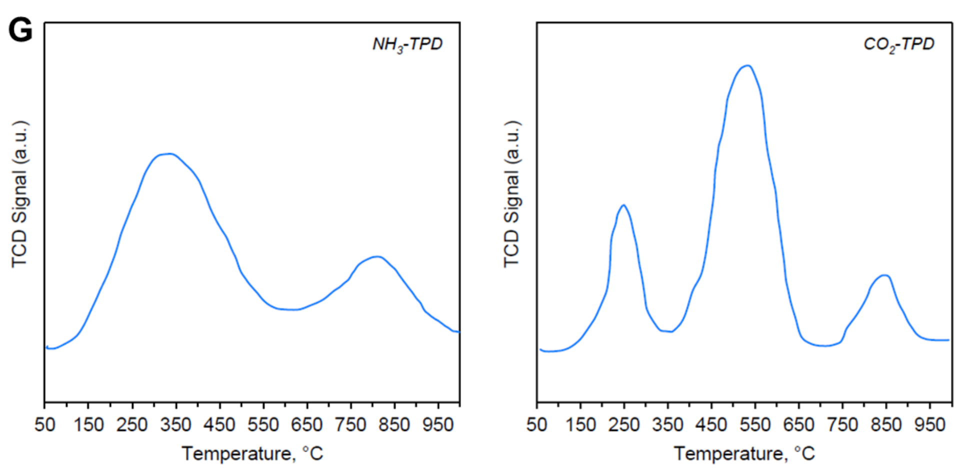
G
NH_3-TPD
TCD Signal (a.u.)
50 150 250 350 450 550 650 750 850 950
Temperature, °C
CO_2-TPD
TCD Signal (a.u.)
50 150 250 350 450 550 650 750 850 950
Temperature, °C

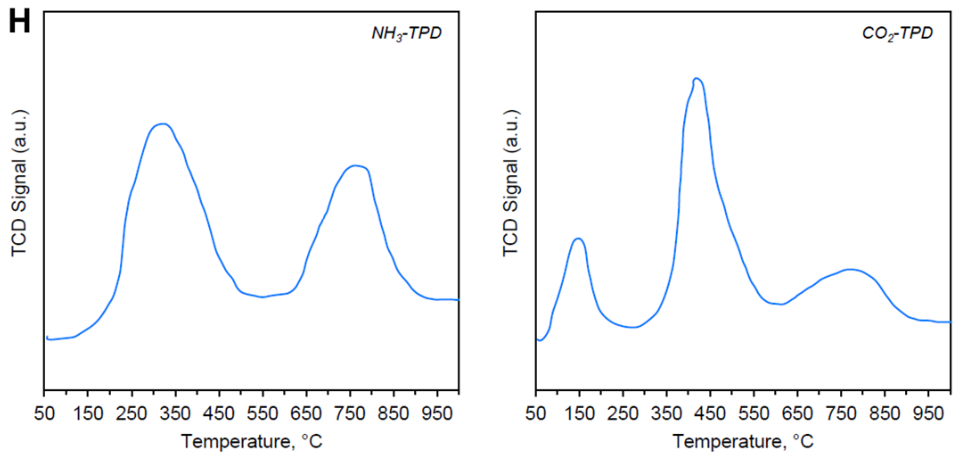
H
NH3-TPD
TCD Signal (a.u.)
50 150 250 350 450 550 650 750 850 950
Temperature, °C
CO2-TPD
TCD Signal (a.u.)
50 150 250 350 450 550 650 750 850 950
Temperature, °C

Table S1. The examined weight percents of first-row transition metals from the total 20 wt% active metal content on hydrotalcite according to the definitive screening design (DSD).

Catalyst Number	Sc	Ti	V	Cr	Mn	Fe	Co	Ni	Cu	Zn
1	50%	100%	100%	100%	100%	100%	100%	100%	100%	100%
2	50%	0%	0%	0%	0%	0%	0%	0%	0%	0%
3	100%	50%	0%	0%	100%	0%	100%	100%	100%	0%
4	0%	50%	100%	100%	0%	100%	0%	0%	0%	100%
5	100%	0%	50%	0%	100%	100%	0%	100%	0%	100%
6	0%	100%	50%	100%	0%	0%	100%	0%	100%	0%
7	100%	0%	0%	50%	0%	100%	100%	0%	100%	100%
8	0%	100%	100%	50%	100%	0%	0%	100%	0%	0%
9	100%	100%	100%	0%	50%	0%	0%	0%	100%	100%
10	0%	0%	0%	100%	50%	100%	100%	100%	0%	0%
11	100%	0%	100%	100%	0%	50%	0%	100%	100%	0%
12	0%	100%	0%	0%	100%	50%	100%	0%	0%	100%
13	100%	100%	0%	100%	0%	0%	50%	100%	0%	100%
14	0%	0%	100%	0%	100%	100%	50%	0%	100%	0%
15	100%	100%	100%	0%	0%	100%	100%	50%	0%	0%
16	0%	0%	0%	100%	100%	0%	0%	50%	100%	100%
17	100%	100%	0%	100%	100%	100%	0%	0%	50%	0%
18	0%	0%	100%	0%	0%	0%	100%	100%	50%	100%
19	100%	0%	100%	100%	100%	0%	100%	0%	0%	50%
20	0%	100%	0%	0%	0%	100%	0%	100%	100%	50%
21	50%	50%	50%	50%	50%	50%	50%	50%	50%	50%

Table S2. The examined weight percents of Fe, Mn, and Ni from the total 20 wt% active metal content on hydrotalcite according to the simplex centroid design (SCD).

Catalyst Number	Fe	Mn	Ni
1	100%	0%	0%
2	0%	100%	0%
3	0%	0%	100%
4	50%	50%	0%
5	50%	0%	50%
6	0%	50%	50%
7	33.33%	33.33%	33.33%
8	66.67%	16.67%	16.67%
9	16.67%	66.67%	16.67%
10	16.67%	16.67%	66.67%

Table S3. Complete results for regression analysis on experimental data from the second-stage SCD experiment.

Measured Responses	Fe		Mn		Ni		Fe×Mn		Fe×Ni		Mn×Ni		Fe×Mn×Ni	
	Coeff.	*p*	Coeff.	*p*	Coeff.	*p*	Coeff.	*p*	Coeff.	*p*	Coeff.	*p*	Coeff.	*p*
$\%TOC_{removal}$ (%)	77.1	0.012	63.4	0.011	22.5	0.011	109	0.012	123.1	0.013	147.7	0.013	-478	0.026
Y_{H2} (%)	15.12	0.01	13.28	0.01	24.48	0.01	28	0.010	143.2	0.011	136.16	0.011	960	0.024
$\%H_2$ (%)	11	0.01	6.55	0.01	18.5	0.01	7.15	0.010	99.05	0.012	88.65	0.012	490	0.028
$CO:H_2$	0.43	0.011	1.16	0.011	0.64	0.01	0.98	0.011	-0.54	0.011	2.9	0.014	-7.8	0.024
SBrA (mmol NH_3/g)	0.77	0.012	0.66	0.012	0.33	0.01	0.88	0.012	0.99	0.013	1.19	0.013	-3.83	0.025
WBrA (mmol NH_3/g)	0.43	0.012	0.36	0.011	0.13	0.011	0.61	0.012	0.69	0.013	0.83	0.013	-2.69	0.024
SLA (mmol NH_3/g)	0.24	0.011	0.54	0.012	0.33	0.011	0.4	0.011	1.18	0.014	0.22	0.011	-3.19	0.023
WLA (mmol NH_3/g)	0.18	0.01	0.17	0.01	0.25	0.011	0.22	0.010	1.12	0.011	1.07	0.011	7.52	0.028
SBS (mmol CO_2/g)	0.28	0.016	0.29	0.016	0.42	0.018	-0.03	0.009	0.05	0.011	0.06	0.011	-0.47	0.026
Phenols conversion	0.75	0.012	0.64	0.012	0.37	0.01	0.82	0.012	1.09	0.013	0.99	0.013	-3.47	0.028
Acid content ($mol.L^{-1}$)	0.46	0.012	0.35	0.011	0.15	0.01	0.62	0.012	0.74	0.013	0.9	0.014	-2.55	0.022

Table S4. Physicochemical properties of ten different catalysts defined by the simplex centroid design protocol in Table S2.

Active Metals	S_{BET} (m^2/g)	d_{BJH} (nm)	V_{BJH} (cm^3/g)	Isotherm and Hysteresis Types	TAS by NH_3-TPD (mmol NH_3/g)	TBS by CO_2-TPD (mmol CO_2/g)
Fe	158.20	8.86	1.14	IV–H1	1.57	0.46
Mn	183.32	7.83	1.11	IV–H1	1.64	0.42
Ni	149.97	8.16	1.18	IV–H1	1.10	0.54
$Fe_{0.5}$-$Mn_{0.5}$	175.44	8.62	1.17	IV–H1	2.06	0.40
$Fe_{0.5}$-$Ni_{0.5}$	166.34	8.2	1.09	IV–H1	2.33	0.50
$Mn_{0.5}$-$Ni_{0.5}$	183.26	8.03	1.10	IV–H1	2.18	0.52
$Fe_{0.33}$-$Mn_{0.33}$-$Ni_{0.33}$	188.93	8.53	1.05	IV–H1	2.20	0.47
$Fe_{0.67}$-$Mn_{0.17}$-$Ni_{0.17}$	203.71	7.98	1.03	IV–H1	2.50	0.46
$Fe_{0.17}$-$Mn_{0.67}$-$Ni_{0.17}$	190.57	8.97	1.03	IV–H1	2.57	0.41
$Fe_{0.17}$-$Mn_{0.17}$-$Ni_{0.67}$	135.91	8.49	1.16	IV–H1	1.96	0.55

Table S5. Active sites composition of ten different catalysts defined by the simplex centroid design protocol in Table S2. Acidic site is expressed as mmol NH_3/g and basic site is expressed as mmol CO_2/g.

Active Metals	**SBrA**	**WBrA**	**SLA**	**WLA**	**TAS**	**SBS**	**MBS**	**WBS**	**TBS**
Fe	0.75	0.42	0.24	0.16	1.57	0.28	0.09	0.09	0.46
Mn	0.63	0.34	0.54	0.13	1.64	0.29	0.06	0.07	0.42
Ni	0.35	0.14	0.33	0.28	1.10	0.42	0.08	0.04	0.54
$Fe_{0.5}$-$Mn_{0.5}$	0.89	0.52	0.49	0.17	2.06	0.28	0.08	0.04	0.40
$Fe_{0.5}$-$Ni_{0.5}$	0.80	0.46	0.58	0.50	2.33	0.36	0.08	0.06	0.50
$Mn_{0.5}$-$Ni_{0.5}$	0.78	0.44	0.49	0.47	2.18	0.37	0.06	0.09	0.52
$Fe_{0.33}$-$Mn_{0.33}$-$Ni_{0.33}$	0.71	0.39	0.45	0.65	2.20	0.32	0.09	0.06	0.47
$Fe_{0.67}$-$Mn_{0.17}$-$Ni_{0.17}$	0.92	0.54	0.43	0.61	2.50	0.30	0.07	0.09	0.46
$Fe_{0.17}$-$Mn_{0.67}$-$Ni_{0.17}$	0.91	0.53	0.49	0.63	2.57	0.30	0.06	0.05	0.41
$Fe_{0.17}$-$Mn_{0.17}$-$Ni_{0.67}$	0.61	0.33	0.46	0.56	1.96	0.39	0.07	0.09	0.55

Table S6. Summary of XPS results for oxidation states and chemical bonds associated with active metals on hydrotalcite.

Impregnated Metals	Binding Energy (eV)	Peak	State
Fe	74.5	Al 2p	Aluminum oxide
	50.5	Mg 2p	Magnesium oxide
	709.6	Fe $2p_{3/2}$	Iron(II) oxide
	710.6	Fe $2p_{3/2}$	Iron(III) oxide
Mn	74.5	Al 2p	Aluminum oxide
	50.5	Mg 2p	Magnesium oxide
	640.5	Mn $2p_{3/2}$	Manganese(III) oxide
	653.3	Mn $2p_{1/2}$	Manganese(IV) oxide
Ni	74.5	Al 2p	Aluminum oxide
	50.5	Mg 2p	Magnesium oxide
	855.6	Ni $2p_{3/2}$	Nickel(II) hydroxide
$Fe_{0.5}$-$Mn_{0.5}$	74.5	Al 2p	Aluminum oxide
	50.5	Mg 2p	Magnesium oxide
	50.5	Mg 2p	Magnesium oxide
	710	Fe $2p_{3/2}$	Iron(II) oxide
	640.5	Mn $2p_{3/2}$	Manganese(III) oxide
	653.3	Mn $2p_{1/2}$	Manganese(IV) oxide
$Fe_{0.5}$-$Ni_{0.5}$	74.5	Al 2p	Aluminum oxide
	50.5	Mg 2p	Magnesium oxide
	709.6	Fe $2p_{3/2}$	Iron(II) oxide
	710.6	Fe $2p_{3/2}$	Iron(III) oxide
	855.6	Ni $2p_{3/2}$	Nickel(II) hydroxide
$Mn_{0.5}$-$Ni_{0.5}$	74.5	Al 2p	Aluminum oxide
	50.5	Mg 2p	Magnesium oxide
	640.5	Mn $2p_{3/2}$	Manganese(III) oxide
	653.3	Mn $2p_{1/2}$	Manganese(IV) oxide
	855.6	Ni $2p_{3/2}$	Nickel(II) hydroxide
Fe_x-Mn_y-Ni_z	74.5	Al 2p	Aluminum oxide
	50.5	Mg 2p	Magnesium oxide
	640.5	Mn $2p_{3/2}$	Manganese(III) oxide
	653.3	Mn $2p_{1/2}$	Manganese(IV) oxide
	855.6	Ni $2p_{3/2}$	Nickel(II) hydroxide
	709.6	Fe $2p_{3/2}$	Iron(II) oxide
	710.6	Fe $2p_{3/2}$	Iron(III) oxide

Table S7. Chemical concentration of the aqueous products from the SCD experiments using ten different catalysts defined in Table S2.

Compounds		Catalyst Numbers Defined from SCD protocol									
		1	2	3	4	5	6	7	8	9	10
***GC-MS* (mM)**	**RT (min)**										
o-cresol	38.8	0.0	0.0	0.0	0.0	0.0	0.0	0.0	0.0	0.0	0.0
3-methyl catechol	44.9	1.1	1.2	0.4	0.7	0.7	1.7	0.7	1.0	1.5	0.2
(2*Z*,4*Z*)-2-methylhexa-2,4-dienedioic acid	56.9	2.4	2.5	0.8	1.4	1.4	3.7	1.4	2.0	3.2	0.4
succinic acid	42.6	29.5	30.3	24.4	22.7	25.8	20.6	24.5	23.3	29.5	21.5
propionic acid	26.1	29.6	22.8	23.7	29.2	23.5	30.3	20.3	30.6	21.8	20.8
2-(5-oxo-2,5-dihydrofuran-2-yl)propanoic acid	56.9	5.9	4.6	4.7	5.8	4.7	6.1	4.1	6.1	4.4	4.2
o-chlorophenol	46.5	0.0	0.0	0.0	0.0	0.0	0.0	0.0	0.0	0.0	0.0
2-chlorohydroquinone	52.5	0.5	1.2	0.3	0.6	0.1	1.2	0.3	0.5	1.1	0.0
(2*E*,4*Z*)-4-hydroxy-6-oxohexa-2,4-dienoic acid	51.6	0.7	0.3	0.9	0.3	1.3	0.5	3.1	1.3	2.1	1.3
2-nitrohydroquinone	56.5	0.7	0.6	0.2	0.1	0.5	0.4	0.3	0.7	0.8	0.1
o-nitrophenol	50.5	0.0	0.0	0.0	0.0	0.0	0.0	0.0	0.0	0.0	0.0
fumaric acid	41.8	18.4	16.1	18.2	16.3	16.5	18.2	19.3	15.1	18.4	17.5
oxalic acid	32.0	3.7	3.2	3.6	3.3	3.3	3.6	3.9	3.0	3.7	3.5
malonic acid	37.3	215.8	248.0	189.5	185.1	221.4	238.7	139.5	162.8	178.7	239.7
acetic acid	20.8	5.4	6.2	4.7	4.6	5.5	6.0	3.5	4.1	4.5	6.0
***Spectrophotometry* (mM)**	**Wavelength**										
hydrogen peroxide	525 nm	0.5	0.2	0.7	0.5	0.4	1.0	0.5	0.4	0.8	0.3
hydrochloric acid	460 nm	135.5	137.3	133.7	143.5	130.5	134.6	149.8	136.4	131.8	144.6
nitric acid	540 nm	134.2	139.4	142.7	144.3	149.1	138.2	150.3	134.4	149.3	135.7
***µGC* (%v/v)**	**RT (min)**										
hydrogen	26.3	7.5	5.5	17.5	8.5	35.0	32.5	35.0	32.5	45.5	37.5
carbon dioxide	37.4	76.0	89.0	58.0	82.2	-5.0	46.4	11.3	6.8	28.6	7.5
carbon monoxide	44.5	16.5	5.5	24.5	9.4	70.0	21.1	53.7	60.7	25.9	55.0

Table S8. Time evolution of concentration of compounds in the aqueous product from semi-continuous processing of 0.15 M *o*-cresol.

200 °C										
Hour(s)	CRE	MCA	MHDA	SUCCI	PROPI	DHFPA	CO_2	CO	H_2	H_2O_2
0	150.00	0.00	0.00	0.00	0.00	0.00	0.00	0.00	0.00	500.00
1	75.00	37.50	31.43	0.61	0.61	3.33	4.29	472.91	573.16	400.00
2	50.00	30.20	21.58	4.69	4.69	4.02	7.62	402.49	333.50	300.00
3	40.00	17.25	11.38	5.69	5.69	4.17	10.58	424.44	450.75	200.00
4	35.00	8.40	7.29	5.69	5.69	4.20	13.36	412.54	438.21	100.00
5	30.00	0.31	5.06	5.69	5.69	4.21	16.02	420.17	454.67	50.00
6	25.00	0.25	4.01	5.69	5.69	4.21	18.58	408.63	459.85	0.00
250 °C										
Hour(s)	CRE	MCA	MHDA	SUCCI	PROPI	DHFPA	CO_2	CO	H_2	H_2O_2
0	150.00	0	0	0.00	0.00	0.00	0.00	0.00	0.00	500.00
1	55.00	37.50	12.75	15.61	15.61	4.99	17.84	509.69	607.86	200.00
2	25.00	30.20	10.40	19.69	19.69	7.00	30.48	425.78	503.18	100.00
3	15.00	17.25	5.75	20.69	20.69	7.70	42.41	298.18	407.57	50.00
4	10.00	8.40	3.60	20.69	20.69	8.00	53.85	255.60	404.18	25.00
5	5.00	0.31	2.17	20.69	20.69	8.00	64.83	247.03	429.15	10.00
6	2.00	0.25	1.86	20.69	20.69	8.00	75.36	271.52	443.72	0.00
300 °C										
Hour(s)	CRE	MCA	MHDA	SUCCI	PROPI	DHFPA	CO_2	CO	H_2	H_2O_2
0	150.00	0.00	0	0.00	0.00	0.00	0.00	0	0	500.00
1	45.00	37.50	10.75	21.09	21.09	8.72	55.35	358.03	587.79	150.00
2	15.00	30.20	8.40	27.09	27.09	11.72	96.55	208.19	317.30	50.00
3	8.00	17.25	3.75	29.09	29.09	12.72	130.92	175.19	449.58	25.00
4	5.00	8.40	1.60	30.09	30.09	13.22	159.61	139.83	461.18	15.00
5	2.00	0.31	0.17	30.59	30.59	13.52	183.58	117.64	500.06	5.00
6	0.00	0.25	0.06	31.09	31.09	13.72	203.64	94.62	523.24	0.00

Table S9. Time evolution of concentration of compounds in the aqueous product from semi-continuous processing of 0.15 M *o*-chlorophenol.

Hour(s)	ONP	NHQ	HODA	FUMA	OXAL	MALO	ACETIC	H_2O_2	CO_2	CO	H_2
200 °C											
0	150.00	0.00	0.00	0.00	0.00	0.00	0.00	500.00	0.00	0.00	0.00
1	110.00	14.00	11.00	10.67	7.40	288.50	0.69	400.00	10.00	324.28	244.55
2	75.00	10.00	10.00	10.67	5.13	287.81	1.38	300.00	17.77	555.59	661.36
3	50.00	9.00	8.00	10.67	3.55	287.12	2.07	200.00	24.70	561.42	587.14
4	30.00	3.00	7.00	10.67	2.46	286.43	2.76	100.00	31.18	573.26	614.58
5	15.00	2.00	6.50	10.67	1.70	285.75	3.45	50.00	37.37	559.77	607.08
6	10.00	1.85	6.25	10.67	1.18	285.06	4.13	0.00	43.36	564.30	609.57
250 °C											
Hour(s)	ONP	NHQ	HODA	FUMA	OXAL	MALO	ACETIC	H_2O_2	CO_2	CO	H_2
0	150.00	0.00	0.00	0.00	0.00	0.00	0.00	500.00	0.00	0.00	0.00
1	100.00	10.00	12.00	6.28	2.71	279.71	7.93	200.00	41.63	328.66	259.35
2	55.00	6.00	11.00	11.28	5.04	262.90	15.75	100.00	71.12	448.83	401.23
3	30.00	4.40	7.60	13.28	3.00	250.21	20.44	50.00	98.96	474.45	530.90
4	15.00	3.48	5.80	14.08	1.50	242.63	25.01	25.00	125.66	411.34	566.85
5	5.00	2.42	4.21	14.18	1.00	237.18	28.47	10.00	151.27	386.28	573.01
6	0.00	2.22	1.15	14.28	1.00	251.83	33.81	0.00	175.84	374.96	588.19
300 °C											
Hour(s)	ONP	NHQ	HODA	FUMA	OXAL	MALO	ACETIC	H_2O_2	CO_2	CO	H_2
0	150.00	0.00	0.00	0.00	0.00	0.00	0.00	500.00	0.00	0.00	0.00
1	65.00	20.00	15.00	18.11	0.00	248.54	33.31	150.00	129.15	245.51	250.79
2	30.00	17.00	12.00	18.11	0.00	219.16	62.68	50.00	225.29	287.38	629.24
3	15.00	15.00	6.00	18.11	0.00	193.26	88.58	25.00	305.48	231.73	585.61
4	5.00	5.00	3.00	18.11	0.00	170.42	111.43	15.00	372.42	194.30	646.80
5	1.00	1.00	2.00	18.11	0.00	150.27	131.57	5.00	428.36	156.72	667.69
6	0.00	0.00	1.00	18.11	0.00	132.51	149.33	0.00	475.15	130.66	693.59

Table S10. Time evolution of concentration of compounds in the aqueous product from semi-continuous processing of 0.15 M *o*-nitrophenol.

200 °C											
Hour(s)	CLP	CLH	HODA	FUMA	OXAL	MALO	ACETIC	H_2O_2	CO_2	CO	H_2
0	150.00	0.00	0.00	0.00	0.00	0.00	0.00	500.00	0.00	0.00	0.00
1	110.00	14.00	8.00	10.67	7.40	288.50	0.69	400.00	10.00	324.28	244.55
2	75.00	15.00	10.00	10.67	5.13	287.81	1.38	300.00	17.77	555.59	661.36
3	50.00	9.00	8.00	10.67	3.55	287.12	2.07	200.00	24.70	561.42	587.14
4	30.00	3.00	7.00	10.67	2.46	286.43	2.76	100.00	31.18	573.26	614.58
5	15.00	2.00	6.50	10.67	1.70	285.75	3.45	50.00	37.37	559.77	607.08
6	10.00	1.85	6.25	10.67	1.18	285.06	4.13	0.00	43.36	564.30	609.57
250 °C											
Hour(s)	CLP	CLH	HODA	FUMA	OXAL	MALO	ACETIC	H_2O_2	CO_2	CO	H_2
0	150.00	0.00	0.00	0.00	0.00	0.00	0.00	500.00	0.00	0.00	0.00
1	100.00	15.00	10.00	6.28	2.71	279.71	7.93	200.00	41.63	328.66	259.35
2	55.00	18.00	9.00	11.28	5.04	262.90	15.75	100.00	71.12	448.83	401.23
3	30.00	11.00	6.80	13.28	3.00	250.21	20.44	50.00	98.96	474.45	530.90
4	15.00	5.80	5.80	14.08	1.50	242.63	25.01	25.00	125.66	411.34	566.85
5	5.00	3.63	5.21	14.18	1.00	237.18	28.47	10.00	151.27	386.28	573.01
6	0.00	2.41	5.15	14.28	1.00	251.83	33.81	0.00	175.84	374.96	588.19
300 °C											
Hour(s)	CLP	CLH	HODA	FUMA	OXAL	MALO	ACETIC	H_2O_2	CO_2	CO	H_2
0	150.00	0.00	0.00	0.00	0.00	0.00	0.00	500.00	0.00	0.00	0.00
1	65.00	20.00	15.00	18.11	0.00	248.54	33.31	150.00	129.15	245.51	250.79
2	30.00	22.00	12.00	18.11	0.00	219.16	62.68	50.00	225.29	287.38	629.24
3	15.00	15.00	6.00	18.11	0.00	193.26	88.58	25.00	305.48	231.73	585.61
4	5.00	5.00	3.00	18.11	0.00	170.42	111.43	15.00	372.42	194.30	646.80
5	1.00	1.00	2.00	18.11	0.00	150.27	131.57	5.00	428.36	156.72	667.69
6	0.00	0.00	1.00	18.11	0.00	132.51	149.33	0.00	475.15	130.66	693.59

Table S11. The list of ordinary differential equations derived from unsteady-state mass balance of the reactants, intermediates, and products.

Components	Differential Equations Derived from Transient Mass Balance
o-cresol	$dC_{CRE}/dt = -r_1$
3-methyl catechol	$dC_{MCA}/dt = r_1 - r_2$
(2*Z*,4*Z*)-2-methylhexa-2,4-dienedioic acid	$dC_{MHDA}/dt = r_2 - r_3 - r_4 - r_5 - r_6$
succinic acid	$dC_{SUCCI}/dt = r_3$
propionic acid	$dC_{PROPI}/dt = r_3$
2-(5-oxo-2,5-dihydrofuran-2-yl)propanoic acid	$dC_{DHFPA}/dt = r_4$
carbon dioxide	$dC_{CO2}/dt = 7\times r_6 + r_{16} + r_{12} + r_{13}$
carbon monoxide	$dC_{CO}/dt = 7\times r_5 + 6\times r_9 - r_{16}$
hydrogen	$dC_{H2}/dt = 14\times r_6 + 7\times r_5 + 5\times r_9 + r_2 - r_3 + r_{16}$
o-chlorophenol	$dC_{CLP}/dt = -r_7$
2-chlorohydroquinone	$dC_{CLH}/dt = r_7 - r_8$
(2*E*,4*Z*)-4-hydroxy-6-oxohexa-2,4-dienoic acid	$dC_{HODA}/dt = r_8 + r_{15} - r_9 - r_{10} - r_{11}$
2-nitrohydroquinone	$dC_{NHQ}/dt = r_{14} - r_{15}$
o-nitrophenol	$dC_{ONP}/dt = -r_{14}$
fumaric acid	$dC_{FUMA}/dt = r_{11}$
oxalic acid	$dC_{OXALIC}/dt = r_{11} - r_{13}$
malonic acid	$dC_{MALONIC}/dt = r_{10} - r_{12}$
acetic acid	$dC_{ACETIC}/dt = r_{12}$
hydrogen peroxide	$dC_{H2O2}/dt = -(r_1 + r_2 + r_3 + r_7 + r_8 + 2\times r_{10} + 2\times r_{11} + r_{14} + r_{15})$
hydrochloric acid	$dC_{HCl}/dt = r_8$
nitric acid	$dC_{HNO3}/dt = r_{14}$

Table S12. The physisorption and chemisorption properties of the optimized catalyst after each cycle.

Cycle	S_{BET} (m^2/g)	SBrA (mmol NH_3/g)	SLA (mmol NH_3/g)	WBrA (mmol NH_3/g)	WLA (mmol NH_3/g)	TAS (mmol NH_3/g)
1	194.25	0.8046	0.4483	0.4588	0.7045	2.4161
2	192.31	0.82	0.4662	0.4451	0.6904	2.4223
3	188.46	0.8371	0.4569	0.4317	0.6628	2.3884
4	184.69	0.8203	0.4614	0.4101	0.6760	2.3679
5	188.39	0.8039	0.4476	0.4101	0.6490	2.3106
6	190.27	0.7959	0.4252	0.3896	0.6425	2.2532
7	186.46	0.8038	0.4167	0.3857	0.6553	2.2616
8	188.33	0.7878	0.4375	0.3703	0.6553	2.2509
9	190.21	0.7799	0.4244	0.3666	0.6488	2.2197
10	192.11	0.7721	0.4372	0.3849	0.6358	2.2300